DAHLGREN DIVISION
NAVAL SURFACE WARFARE CENTER

Silver Spring, Maryland 20903-5640

HYPERVELOCITY WIND TUNNEL NO. 9 MACH 7 THERMAL STRUCTURAL FACILITY VERIFICATION AND CALIBRATION

BY JOHN F. LAFFERTY   DANIEL E. MARREN

STRATEGIC AND SPACE SYSTEMS DEPARTMENT

JUNE 1996

19971006 051

DTIC QUALITY INSPECTED 3

REPORT DOCUMENTATION PAGE

1. AGENCY USE ONLY (Leave blank)	2. REPORT DATE	3. REPORT TYPE AND DATES COVERED
	June 1996	Final

4. TITLE AND SUBTITLE

Hypervelocity Wind Tunnel No. 9 Mach 7 Thermal Structural Facility Verification and Calibration

5. FUNDING NUMBERS

6. AUTHOR(s)

John F. Lafferty, Daniel E. Marren

7. PERFORMING ORGANIZATION NAME(S) AND ADDRESS(ES)

Commander
Naval Surface Warfare Center
Dahlgren Division (Code K24)
17320 Dahlgren Road
Dahlgren, VA 22448-5100

8. PERFORMING ORGANIZATION REPORT NUMBER

NSWCDD/TR-95/231

9. SPONSORING/MONITORING AGENCY NAME(S) AND ADDRESS(ES)

10. SPONSORING/MONITORING AGENCY REPORT NUMBER

11. SUPPLEMENTARY NOTES

12a. DISTRIBUTION/AVAILABILITY STATEMENT

Approved for public release; distribution is unlimited.

12b. DISTRIBUTION CODE

13. ABSTRACT (Maximum 200 words)

This report summarizes the verification and calibration of the new Mach 7 Thermal Structural Facility located at the White Oak, Maryland, site of the Dahlgren Division, Naval Surface Warfare Center. This effort was in support of the development of a thermal structural ground testing capability for interceptor seeker windows and radomes. The new facility is located in the Hypervelocity Wind Tunnel No. 9 complex and uses common gas supply and vacuum source hardware. Test included the initial facility operation as well as a detailed calibration at three specific design points. Calibration data were collected using a Pitot-probe rake and a blunt sphere cone, each mounted at multiple locations in the test cell to fully characterize the test environment.

The Thermal Structural Facility achieves Mach 7 flow conditions with freestream pressures and temperatures equivalent to ambient pressures and temperatures for altitudes between 38,000 and 67,000 ft (11.5 and 20.5 km) for test times up to 5 sec. This ground test facility provides the capability necessary to test full-scale intercepter seeker windows in a true aero-thermal environment without the need for scaling.

14. SUBJECT TERMS

blowdown facility, wind tunnel, flow restrictor, diaphragm, particle separator, fixed-angle testing, shakeout, calibration, thermocouple, pressure transducer, supersonic flow, inviscid core

15. NUMBER OF PAGES

78

16. PRICE CODE

17. SECURITY CLASSIFICATION OF REPORTS	18. SECURITY CLASSIFICATION OF THIS PAGE	19. SECURITY CLASSIFICATION OF ABSTRACT	20. LIMITATION OF ABSTRACT
UNCLASSIFIED	UNCLASSIFIED	UNCLASSIFIED	UL

NSN 7540-01-280-5500

DTIC QUALITY INSPECTED 3   i/ii

Standard Form 298 (Rev 2-89)
Prescribed by ANSI std. Z39-18
298-102

FOREWORD

This report documents the shakeout and calibration of the new Mach 7 Thermal Structural Facility located at the White Oak, Maryland site of the Dahlgren Division, Naval Surface Warfare Center. This effort was sponsored in part by the Ballistic Missile Defense Organization (BMDO) to support interceptor test and evaluation. The primary objective was to provide a test capability for full-scale seeker window/radome aero-thermal/structural and aero-optical ground testing. This capability complements the existing Mach 8, 10, 14, and 16.5 aerodynamic testing capabilities in Tunnel 9 which support interceptor missile development.

The design and fabrication of facility hardware began in the summer of 1993 with the assembly and initial checkouts occurring in the spring of 1994. The calibration of the Tunnel 9 Thermal Structural Facility was completed during February, 1995. Completion of this upgrade was the result of an outstanding team effort from every member of the Aerodynamic Facilities Branch, K23, and the Aerodynamics Branch, K24. Special acknowledgement also goes to the sponsors, Col. Michael Toole, Director of BMDO T&E, Ms. Kathleen Ruemmele, Asst. Dir. of Test Resources, Mr. Donald McClure of the THAAD Project Office and Dr. Eric Hedlund/Mr. Chester DeCesaris, Program Managers of BMDO Ground Test Facilities.

Approved by:

D. B. COLBY, Head
Strategic and Space Systems Department

CONTENTS

ILLUSTRATIONS

ILLUSTRATIONS (Continued)

TABLES

TABLES (Continued)

GLOSSARY

B	Bias Error at 95 percent confidence level
c_p	Heat capacity / specific heat of nitrogen (0.248 BTU/lbm-deg R)
C_p	Pressure coefficient, $(P - P_\infty)/q_\infty$
k	Thermal conductivity
Mach	Freestream Mach number
P	Precision error at 95percent confidence level, $(t_{95}S)$ or pressure, (general)
P[A-G][1-8]	Cone surface pressure, ray and station number
Pamb, P_{amb}	Ambient pressure at a given altitude
Pinf, P_∞	Freestream pressure
P0, P_0	Supply pressure
Pitot, PT	Pitot pressure
P_w	Wall surface pressure
$\dot{Q}$	Heat transfer rate
qinf, q_∞	Freestream dynamic pressure
Reinf, Re/L	Freestream unit Reynolds number
ρ	Density
RHOinf, ρinf, ρ_∞	Freestream density
S	Sample standard deviation
T[A-G][1-8]	Cone surface temperature, ray and station number
Tamb, T_{amb}	Ambient pressure at a given altitude
TBS[1-8]	Backside thermocouple and station number
T_H	Heater temperature
Tinf, T_∞	Freestream temperature
T0, T_0	Supply temperature
T_w	Wall surface temperature
t_{95}	Student's "t" distribution for a 95percent confidence level
Uinf, U_∞	Freestream velocity
U_{rss}	Uncertainty, $[B^2 + P^2]^{1/2}$

INTRODUCTION

The Hypervelocity Wind Tunnel No. 9 (Tunnel 9) Thermal Structural Facility located at the White Oak, Maryland site of the Dahlgren Division, Naval Surface Warfare Center was built to provide data to support endo-atmospheric interceptor seeker window/radome testing. The objective of this facility is to produce a duplicated Mach 7 flight environment in a ground test facility with freestream pressures and temperatures equal to the ambient atmospheric pressures and temperatures for altitudes between 38,000 and 67,000 ft (11.5 and 20.5 km) and for test times up to 5 seconds (Reference 1). The intent of the facility development was to duplicate the thermal shock, peak heating, and thermal heat soak of flight to assess the thermal, structural and optical response of full-size seeker windows and radomes. The verification of a flight quality seeker window in a ground test facility prior to a flight test can greatly reduce the risk to the system by identifying problems with an initial design or by verifying the survivability and performance of a final design.

This report describes the important facility development areas and documents the results from the verification and calibration of the Tunnel 9 Thermal Structural Facility that concluded in February 1995. Data presented in this report verifies facility performance and defines the usable inviscid test core for three specific design points.

TUNNEL 9 FACILITY DESCRIPTION

Tunnel 9 is a blowdown facility which uses pure nitrogen as the working fluid and currently operates at Mach numbers of 7, 8, 10, 14, and 16.5. Ranges for Reynolds numbers, supply conditions, and run times for current facility operation are listed in Table 1. The test section is over 12 ft long and is 5 ft in diameter, which enables testing of full-scale reentry and intercepter configurations. A layout of Tunnel 9 is shown in Figure 1.

During a typical run, the vertical heater vessel is used to pressurize and heat a fixed volume of nitrogen to a predetermined pressure and temperature. The test cell and vacuum sphere are evacuated to approximately 1 mmHg and are separated from the heater by a pair of metal diaphragms. When the nitrogen in the heater reaches the desired temperature and pressure, the diaphragms are ruptured. The gas flows from

the top of the heater, expanding through the contoured nozzle into the test section at the desired test conditions. As the hot gas exits the top of the heater, cooler nitrogen gas from the pressurized driver vessels enters the heater base. The cold gas drives the hot gas out the top of the heater in a piston-like fashion, thereby maintaining constant conditions in the nozzle supply plenum and the test section during the run. A more complete description of the Tunnel 9 capabilities can be found in Reference 2.

Tunnel 9 was originally planned as three separate wind tunnels, or legs, that would all use a common high pressure nitrogen source and vacuum sphere. The north and center legs both were designed with vertical heater vessels and the south leg with a horizontal heater vessel. Prior to this upgrade only the north leg was used for testing. Some existing center leg hardware from the original construction of Tunnel 9 was used in the development of the Mach 7 Thermal Structural Facility, greatly reducing facility development cost and time.

THERMAL STRUCTURAL FACILITY DESCRIPTION

Development of the Mach 7 capability included three major efforts: the heater, the diaphragm area and the nozzle. The design philosophy for this upgrade was to use existing hardware and design methodology where possible to limit the development cost and time. This development required the assembly of the center leg heater and the fabrication of a new diaphragm area and nozzle. The effort also required the repositioning of some large-diameter piping to connect the test cell to the vacuum sphere.

CENTER LEG HEATER

The center leg heater is identical in design to the heater used in the north leg except for the bottom end-closure plug. Figure 2 shows the heater, a nominal 17 ft^3 pressure vessel that is insulated from the hot gas by a carbon/graphite composite liner package. The design goals for the heater were to achieve pressures up to 27,000 psi at 3400°F. North leg heater bottom end-closure hardware had been modified, reducing its maximum operational pressure capability to 22,000 psi in that leg. The center leg bottom end-closure was not modified and retains the full pressure rating necessary to achieve 27,000 psi. Assembly and pressure checking of the vessel were the major efforts required to complete the center-leg heater development. This required a series of pressure leak tests and an acoustic emissions test to 110 percent of the desired running pressure. These tests were successfully completed, certifying the vessel for normal operations at pressures up to 27,000 psi.

DIAPHRAGM AREA AND FLOW RESTRICTOR

The diaphragm area of the tunnel, as shown in Figure 3, contains the flow restrictor, two diaphragms and a particle separator just upstream of the nozzle settling chamber or plenum. This assembly is nearly identical to the Mach 14 assembly with the exception of the flow restrictor. To achieve the necessary run time in the facility, more mass was required in the heater than at Mach 14. This additional mass is achieved by running the heater at higher pressures than are required in the plenum and throttling the pressure down through a sonic orifice flow restrictor to the desired plenum supply pressure. The flow restrictor design for the Thermal Structural Facility is required to withstand a pressure differential of 14,000 psi at temperatures of 3400°F for run times up to 6 sec.

The initial flow restrictor design was identical in size and concept to the Mach 14 hardware, having five holes, but was manufactured from a tantalum-10% tungsten alloy. This hardware was only used during the initial three shakeout runs because of structural cracking in the part due to the high thermal gradients and structural loads.

The final design, shown in Figure 4, has a single hole flow-path that is assembled from eight components. This design required additional engineering that included substantial testing and evaluation. The main flow restrictor body that carries the pressure drop is machined from columbium C-103. This part is semi-insulated from the hot flow by three columbium C-103 liners. These liners are designed to reduce heating to the main body and prevent the deformation of the main load-bearing part due to extended high-temperature exposure. The orifice size required to achieve a 14,000 psi pressure drop is a function of the upstream pressure and requires a different ablator seat for each heater pressure operating condition. These seats are machined from tantalum-10% tungsten. Tantalum-10% tungsten can be used in this smaller application because of the more uniform elevation to 3400 °F, reducing the thermal gradients. The flow restrictor also incorporates a Delrin ablator plug that further restricts the open area prior to flow establishment. The Delrin plug ablates during the initial flow of gas and prevents the rarefaction wave, which emanates from the diaphragm burst, from traveling upstream into the heater and damaging the heater element and liner. The liners, ablator seat and Delrin are held in the main restrictor body by two end plates. The upstream plate is machined from columbium C-103 while the downstream plate is tantalum-10% tungsten. Together the flow restrictor assembly meets the requirements to withstand a 14,000 psi pressure differential at 3400 °F for up to 6 sec.

MACH 7 NOZZLE

The third area of design was a nozzle that achieves freestream velocities of 6560 ft/s (2 km/s), approximately Mach 7. Other Tunnel 9 nozzles have length to exit diameter ratios between 7 and 8. This design criteria, which has produced uniform flow

at the nozzle exit of the existing Tunnel 9 nozzles, was maintained for the Mach 7 design. A new Mach 7 contour was generated using a method of characteristics nozzle design code described in References 3 and 4. The Mach 7 nozzle, shown in Figure 3, is 87.75 in. in length from the throat, with an 11.3-in. exit diameter and operates as an open jet into a 5-ft diameter test cell. The nozzle is fully contoured and has a 1.02-in. nozzle throat diameter, which is similar to the Mach 14 nozzle throat (1.1 in. in diameter), thereby maintaining similar mass flow rates through the heater package.

DIFFUSER PIPE HARDWARE AND TEST CELL

Center leg operation required the movement of a 48-in. vacuum sphere isolation valve and approximately 120 ft of 4-ft diameter diffuser pipe from the south leg. Because the Mach 7 nozzle is only about 7 ft in length, as opposed to the 40-ft Mach 10 and 14 nozzles, an additional 33 ft of diffuser pipe extension was required. This extension was welded to the end of the existing pipe to make up the difference, since the locations of the heater and sphere are fixed.

The Thermal Structural Facility schematic is shown in Figure 5. The test cell is 5 ft in diameter and has optical access from both sides as well as from the top. Test models are supported by a sector and sting assembly that allows fixed-angle testing between -5 and 25 deg.

SHAKEOUT AND CALIBRATION TEST OBJECTIVES

Shakeout and calibration of the Thermal Structural facility consisted of the characterization of three design points. Design points 1, 2 and 3 correspond to the duplication of a Mach 7 flight environment at approximate altitudes of 67,000, 51,000 and 38,000 ft (20.5, 15.5 and 11.5 km) respectively. These three altitude points were chosen to span the Mach 7 low endo-atmospheric flight regime where aerothermal loads are significant. Table 2 lists each design point and the corresponding achieved altitude duplication, ambient pressure and ambient temperature. The following sections describe the objectives of each phase of the calibration and the necessary hardware to verify and quantify the quality of the test section core flow.

RAKE OBJECTIVES

The objectives for this phase of the shakeout and calibration were the verification of facility performance and definition of the inviscid core flow at the three different design points. Measurements of supply pressure and temperature as well as test cell Pitot

pressure were used to determine whether a velocity of 6560 ft/s (2 km/s) was achieved at ambient atmospheric pressures and temperatures corresponding to altitudes between 38,000 ft (~11.5 km) and 67,000 ft (~20.5 km) based on the 1962 standard atmosphere. The inviscid core definition was determined from the rake Pitot measurements. These measurements quantified uniformity profiles both spatially and temporally from which the size of the usable core was determined.

CONE OBJECTIVES

The objective of this phase of the calibration was to verify the ability to run an interceptor full-scale forecone and window. This was accomplished by verifying the uniformity of the flow field around a cone, based on cone surface pressure and heat transfer measurements, as well as the ability to duplicate the same flowfield on one side of a cone when it was mounted off-centerline. This capability to test off-centerline will allow the testing of larger full-scale seeker windows that would not fit in the inviscid core if the model was mounted on-centerline.

MODEL HARDWARE

RAKE HARDWARE

The rake, shown in Figure 6, is a wall-mounted 10-deg half-angle wedge that supports up to 71 Pitot tubes. The individual probes are 0.70-in. long with a 0.113-in. outer diameter and are spaced every 0.50 in. Figure 6 shows the orientation of the rake and the probe nomenclature. The rake was placed at two axial stations in the test cell, 0.75 and 15.75 in. downstream of the nozzle exit. The Pitot probes were manufactured from tantalum and the rake leading edge from columbium C-103 in order to withstand repeated exposure to the extreme flow temperatures. It was also necessary to install an air cooling line into the instrumentation cavity to prevent thermal damage to the instrumentation and electrical connections. The cooling line was a perforated 0.25-in. diameter copper tube that injected air into the instrumentation cavity. A regulator was used to maintain a 40-psi plenum pressure inside the cooling line throughout the run cycle. Figure 7 shows a cross sectional schematic of the rake hardware setup.

CONE MODEL HARDWARE

A 15-deg half-angle cone model with a 0.866-in. nose radius was tested. The cone was divided into two sections, a 6-in. base diameter front section and a 9.25-in. base

diameter aft frustra. The model was manufactured from 17-4PH stainless steel with a wall thickness of 0.50 in.

The cone was mounted on a 3.0-in. outer diameter (OD) sting assembly that connected to the base of the front cone section. The aft frustra was split into two equal sections for ease of installation. The sting/sector assembly positioned the cone approximately 0.75 in. downstream of the nozzle exit and allowed for vertical adjustments of 0, 1.25 and 2.5 in. below tunnel centerline. The cone could be moved off-centerline without disconnecting any instrumentation or removing the cone from the sting. The cone was tested on the tunnel centerline as well as 2.5 in. below centerline. Figure 8 shows the model, sting and test cell assembly with the cone mounted 2.5 in. below centerline.

INSTRUMENTATION

TUNNEL INSTRUMENTATION

The instrumentation used to monitor the wind tunnel conditions included one transducer to measure supply pressure (P_0), two thermocouples to measure supply temperature, and Pitot measurements in the test cell. The supply pressure transducer was either a Viatran 304 (S/N 663777) with a 0-10000 psi range or a Viatran 121 (S/N 665462) with a 0-20000 psi range. The two supply temperature (T_0) thermocouples are redundant and are averaged. Both supply-temperature thermocouples were fabricated at Tunnel 9 using tungsten-5% rhenium vs tungsten-26% rhenium wire, which have a useful range up to 4200 °F. All Pitot measurements were made using Kulite XT-140-200a transducers mounted either in the Pitot rake or one mounted in the cone model nose tip. Also the test cell wall pressure was measured using a 0-5 psia Microswitch transducer. This transducer port was located on the wall of the 60-in. diameter test cell at the same axial location as the nozzle exit, and measured the static pressure in the recirculation region outside the test core.

RAKE INSTRUMENTATION

The rake was instrumented with 33 Pitot probes. Pressure in each probe was measured with a Kulite XT-140-200a pressure transducer with a 0-200 psia useful range. The Pitot probes were designated by the letters "PT" followed by a number as shown in Figure 6. The even-number probes (PT2, PT4, PT6, ...) were those above the tunnel centerline and the odd-number probes (PT1, PT3, PT5, ...) were below the centerline. PT0 was positioned within one probe radius of the tunnel centerline. Also, a Type E beaded thermocouple was tack-welded to the inside of the instrumentation cavity at the center of the rake to monitor the thermal heat soak during the run as well

as after to account for thermal drift and survivability of the pressure transducers. No thermal drift was observed during any run and all gauges survived post-run thermal heat soak temperatures up to 500°F.

CONE INSTRUMENTATION

The cone was instrumented with both pressure and temperature gauges to assess the uniformity of the cone flowfield. The instrumentation layout, positions and nomenclature are shown in Figure 9. The top side of the model was heavily instrumented to allow the mapping of the boundaries of the uniform flow region when the full cone was mounted off-centerline. Looking downstream, the right side was dedicated to pressure instrumentation every 30 deg while the left side was dedicated to temperature gauges every 30 deg.

The cone surface pressures were measured with Kulite XT-140-50a, 0-50 psia, pressure transducers with the exception of the stagnation pressure port that used a Kulite XT-140-200a, 0-200 psia transducer. Pressure transducers were threaded and sealed into brass mounting adapters. The adapters were cemented using Loctite adhesive No. 271 to 0.62-in. inner diameter (ID) pressure tubing that was installed normal to the model surface. Tubing lengths were nominally 2-3 in.

The cone surface temperatures were measured using Medtherm Type E coaxial thermocouples, model TCS-E-10370. These thermocouples have an OD of 0.062 in. and are 0.5 in. in length, matching the model wall thickness of 0.5 in. The coaxial gauges are constructed from a chromel outer jacket that surrounds an insulated constantan center wire. This assembly is cemented into the 0.063-in. diameter hole normal to the surface using Loctite RC/620 high-temperature retaining compound. The thermocouple was sanded at the surface to conform with the external contour as well as to form the thermal junction. The data from these gauges were used to determine the heat transfer rate on the model surface based on a one-dimensional heat transfer analysis. Also, 7 Type E beaded thermocouples were tack-welded to the inside wall of the model at each of the instrumentation stations 2 through 8 between rays A and H. These backside thermocouples were labeled TBS2-TBS8 corresponding to stations 2-8.

TEST PROCEDURE

RUN PROCEDURE

Preparations for each run began with the positioning of either the calibration rake or calibration cone followed by the securing of the test cell and tunnel room. The heater vessel was then charged to its initial pressure, and pressurization of the driver vessels was begun. Calibrations of the pressure instrumentation were then performed. First, the tunnel supply-pressure transducer was calibrated in place. A series of shunt resistances simulating known pressures were applied to the P_0 transducer, and the output recorded, allowing a calibration curve to be computed. Calibrations of pressure transducers in the test cell and model were then performed by recording data during the evacuation of the test cell from atmospheric pressure down to approximately 1 mmHg. Two MKS Baratron-type 145 transducers with ranges of 1000 and 10 mmHg monitor the test cell pressure and were used as the working standards. The evacuation process was halted briefly when calibration data were recorded to ensure uniform pressure in the test cell. A static tare was recorded toward the end of the heating cycle, approximately 2 min. before the run to account for any thermal electrical drift in each gauge. When the desired conditions were reached in the heater, the tunnel run was initiated by bursting the two metal diaphragms. Flow was established and data were collected.

For all the runs, the model was held in place with no variation to the model angle-of-attack or position. Each run lasted between 2 and 6 sec, determined by when all preheated hot gas was exhausted from the heater. Following the useful run segment, the control valves are closed and supersonic flow breaks down after approximately 30 to 45 sec. This is immediately followed by a heater cooling cycle that bleeds nitrogen into the heater to cool the heater element and insulation package. As a result of this cooling, hot subsonic nitrogen at approximately 500-800 °F is bled through the nozzle into the test cell for approximately 20-25 min.

DATA ACQUISITION

Data were sampled and recorded using the Tunnel 9 Data Acquisition and Recording Equipment (DARE) VI. DARE VI is a simultaneous-sample-and-hold, single-amplifier-per-channel system with 14-bit resolution. The output signals of all the instrumentation were amplified and fed through six-pole low-pass Bessel filters with a cutoff frequency of 25 Hz before being recorded. The analog filters removed most 60-Hz electrical noise. The sample rate was nominally 500 samples per second per channel for all runs.

DATA REDUCTION

All acquired data were reduced except for the few gauges found to be inoperative. A list of inoperative instrumentation for each of the primary calibration runs is presented in Table 3.

Digital Filtering

In addition to the analog filters used on all channels, data were filtered during reduction to engineering units using a low-pass, sixth-order Butterworth digital filter with a cutoff frequency of 10 Hz except for the cone model thermocouples. The filtering was used for the tunnel supply pressure and temperature, the test cell Pitot data and the cone model pressure data. The data were filtered both forward and backward to prevent the introduction of a time lag.

Tunnel Conditions

The supply and Pitot pressures were determined from their respective calibrations, as outlined above. The supply temperature was determined from the National Institute of Standards and Technology (NIST) tables, Reference 5, for tungsten-5% rhenium vs tungsten-26% rhenium. The tunnel conditions were calculated from these quantities using the procedure outlined in Reference 6. This procedure assumes an isentropic nozzle expansion from the measured supply conditions to the freestream values. An initial guess for the Mach number is made. Using the guessed Mach number, and a measured Pitot pressure, freestream conditions are obtained from perfect gas relations. Using the thermodynamic properties from the standard Mollier diagram for nitrogen and the measured supply conditions, a value of total enthalpy is obtained. A freestream velocity is then obtained based on the conservation of total enthalpy. This value of velocity is converted to Mach number and is compared to the guessed Mach number value. When these two agree, the calculation is complete and the tunnel conditions are known. Otherwise, a new value for Mach number is tried and the iteration procedure continues until convergence is obtained. This method accounts for high pressure and high temperature effects in the supply area.

Pressure Data

All pressure data were reduced into units of pounds-per-square-inch based on the calibration points taken during tunnel evacuation as discussed above.

The Pitot rake pressure data were used to calculate the local tunnel conditions (Mach, P_∞, T_∞, q_∞, Re /L, ρ_∞, U_∞) as described in the previous section and Reference 6.

Also, a normalized form of each tunnel parameter was calculated for each probe based on the average of the same parameter from two probes equally spaced on either side of the tunnel centerline. This average value was calculated using PT13 and PT14 for rake runs 2493, 2496 and 2506, when the rake was mounted 0.75 in. from the nozzle exit, and using PT7 and PT8 for runs 2497 and 2498, when the rake was mounted 15.75 in. downstream of the nozzle exit. These two pairs were chosen to normalize the profiles, because they were representative of where a test cell Pitot strut might be located still within the core flow far from the center. The normalized tunnel conditions were used to determine the relative percent difference of each parameter within the core flow.

The cone pressure data were also converted into the nondimensional forms of P/P_∞ and pressure coefficient, Cp, defined as $(P_w - P_\infty)/q_\infty$. All comparisons of cone pressure data in this report are made in the form of Cp.

Heat Transfer Data

The cone was instrumented with 42 chromel-constantan coaxial thermocouples without cold junction compensators. The millivolt output of each thermocouple was converted to absolute temperature based on the initial reference temperature of the two backface thermocouples, TBS2 and TBS6 that were recorded using cold junction compensators. The model was assumed to be at a uniform temperature giving an initial millivolt level, the average of TBS2 and TBS6, for each gauge. This initial millivolt level was added to the millivolt rise of each gauge. The absolute wall temperature, T_w, was determined from the absolute millivolt level based on the NIST conversion table for a Type E thermocouple.

A heating rate was computed from the temperature history of each gauge using a finite-difference solution to the unsteady, one-dimensional heat-conduction equation for a homogeneous planar slab of finite thickness as described in Reference 7. The thermocouples were mounted in 17-4 PH stainless steel model with a wall thickness of 0.5 in. Calculations were made using 100 evenly spaced node points in the slab, cylindrical coordinates, and temperature-dependent thermal properties.

The properties, thermal conductivity and specific heat, of 17-4 PH stainless steel, chromel, and constantan are all similar at room temperature. However, in the range of operation, approximately 50 to 500 °F, a variation in thermal properties exists. The thermal properties of the system are dominated by the chromel outer jacket of the gauge and the stainless steel in which it is mounted. Preliminary numerical investigations were made using an approximate finite element model using the ABAQUS code to evaluate the effect of each material on the whole system. The results suggest that the gauge temperature measurement is initially dominated by the chromel properties. However during long run times, greater than 1 to 2 sec, the effect of the

surrounding 17-4PH stainless steel becomes more pronounced. The true properties of the gauge setup as used in the test are a combination of the three metal properties, the Loctite interface between the gauge and the model and the local heating rate.

During the numerical investigation the surface heat transfer was back-calculated from the ABAQUS model surface temperature output to a known heat flux input. The heat transfer was then calculated using the ABACUS output as an input to the 1-D homogeneous-variable thermal properties heat conduction data reduction code and was compared to the known input to the ABACUS model. Two cases were investigated, one using the thermally varying chromel properties in the data reduction code and the other using thermally varying stainless steel properties in the same code. This exercise bounded the problem and accounted for the temperature variations in thermal properties of a homogeneous material. It was determined that the chromel variable properties best track the initial rise associated with a step input in heat transfer, similar to a tunnel run start-up. This agrees with the fact that the gauge is mostly chromel which dominates the heat conduction at the measurement junction, located at the center of the coaxial thermocouple. Based on the previous arguments, chromel temperature-dependent properties were chosen for data reduction and are defined as follows:

Thermal Conductivity	$k = 2.43 \times 10^{-4} + 1.06 \times 10^{-7}\, T + 2.65 \times 10^{-11}\, T^2$	(BTU/in.-sec-°F)
Specific Heat	$c_p = 0.104 + 3.40 \times 10^{-5}\, T$	(BTU/lbm-°F)
Density	$\rho = 0.315$	(lbm/in.³)

The estimated uncertainty is ±6 percent which includes the effect of the uncertainty in material thermal properties. All gauges were reduced identically, therefore comparisons and differences between gauges are valid.

In summary, the temperature-dependent thermal properties of chromel were used in the 1-D heat conduction data reduction. The backface temperature rise was negligible; thus, a zero heat flux backface boundary condition was assumed. The measured temperature at the heated surface provided the remaining boundary condition needed to compute the temperature distribution through the slab. Temperatures were calculated at 100 node points accounting for the varying thermal properties of chromel. The heat transfer rate, $\dot{Q}$, was computed from the temperature gradient at the surface and the thermal conductivity of the material. The heating rate was also reduced to dimensionless Stanton number defined as:

$$St = \frac{\dot{Q}}{\rho_\infty U_\infty c_p (T_0 - T_W)}$$

where,

ρ_∞ = freestream density
U_∞ = freestream velocity
c_p = heat capacity of nitrogen

T_0 = measured supply temperature
T_w = measured wall temperature

All comparisons of cone surface heating rates in this report are made in the form of Stanton number.

Photographic Data

Photographic data for center leg testing required a portable Schlieren system consisting of two portable 3-ft diameter optical quality mirrors with identical 12-ft focal lengths. Because of the close proximity of the test cell window to the blast wall that separates the heater and tunnel rooms, the mirrors needed to be positioned with a separation distance of approximately 60 ft. A dual light source was mounted to the blast wall on the south side of the tunnel and shadowgraph collecting optics and two cameras were mounted on the north side of the tunnel. This system allowed for the simultaneous recording of video at standard rates and 70-mm film at approximately 10 frames per second. IRIG-B timing marks were recorded on both images as well as the DARE system, allowing for the correlation of all data.

Experimental Uncertainty

Experimental uncertainties were estimated using principles described in Reference 8, using specific procedures for Tunnel 9 given in Reference 9. In general, the uncertainty in a measurement was composed of a combination of a fixed error or bias, B, and a random error or precision, P. The root-sum-square model was used to estimate the uncertainties at the 95 percent confidence level:

$$U_{rss} = \pm [B^2 + P^2]^{1/2} = \pm [B^2 + (t_{95}S)^2]^{1/2}$$

where U_{rss} is the uncertainty, S is the sample standard deviation, and t_{95} is the 95th percentile point for the two-tailed student's "t" distribution (95-percent confidence interval). Since the sample size for all measurements was greater than 30, t_{95} is considered to be equal to 2. Bias and precision errors were propagated through to calculated parameters individually, then combined into overall uncertainties using the method given in Reference 10. Traceability of working standards to the National Institute of Standards and Technology is maintained through the Navy Metrology and Calibration Program and manufacturer provided calibrations. Estimated uncertainties for the measured tunnel conditions are presented in Table 4. Estimated uncertainties of calculated tunnel conditions are presented in Tables 5-7. The rake runs measured only tunnel conditions, therefore, Tables 5-7 represent the uncertainty associated with all the rake run data at each design point tested. Tables 8 and 9 show the estimated uncertainties associated with both measured and calculated cone data collected during

the cone phase of the calibration. On all data plots presented in this report, uncertainty bands are indicated unless they are smaller than one symbol size.

DISCUSSION

A total of 22 runs were completed during the initial shakeout phase of the center leg Mach 7 capability. Table 10 lists the run log for these 22 runs. The initial 16 runs were used to characterize the performance of the flow restrictor while slowly increasing the heater and supply pressure to the desired levels associated with three specific design points. Each design point corresponds to a specific ablator seat, restrictive orifice, and a maximum P_0 that is defined when the maximum allowable pressure drop, 14,000 psi, is achieved across the flow restrictor assembly. The rake hardware was in place for all 16 initial runs; however, only five runs define the flow quality for the three design conditions.

Table 11 lists the measured supply and determined test cell conditions for runs 2493, 2496, 2497, 2498 and 2506 that define each of the design points 1, 2 and 3. Design points 1 and 2 were both fully defined by runs with the rake in the forward and aft positions on different runs. Design point 3 was sampled only at the forward station, 0.75 in. downstream of the nozzle exit. Design points 1 and 2 were then repeated for six calibration cone runs with the model on- and off-centerline. These six runs are the cone calibration runs and are listed in Table 12. All analysis and discussions of calibration data are limited to these five rake runs and six cone runs.

PITOT RAKE CALIBRATION

Performance Verification

The first stage in the calibration of the facility was the verification of the predicted performance goals. For thermal structural measurements, performance is measured by the ability to produce flight conditions for a specific heat soak time.

In order to duplicate flight, the facility must provide a flow velocity nominally equal to 6560 ft/s (2 km/s), test cell freestream pressure and temperature must match ambient conditions at altitude, and the run times must be on the order of those required for thermal heat soak. Table 2 lists representative design point ambient pressures and temperatures based on the 1962 standard atmosphere.

Figures 10a, 11a and 12a are plots of measured tunnel conditions versus time after diaphragm burst. Supply pressure (P_0) and supply temperature (T_0) are plotted on the left-hand axis while freestream Pitot pressure is shown on the right-hand axis. The diaphragms are burst and a finite period of time exists for the Delrin plug to ablate. During the ablation process, flow is established. P_0 rises to a nearly constant level for the remainder of the run until hot heater gas is exhausted and the driver vessel control valves are closed. This constant P_0 run time is 6, 4 and 2 sec for design points 1, 2 and 3, respectively. Figures 10a, 11a and 12a also show that for the same 6-, 4- and 2-sec constant P_0 run times, the supply temperature starts at a value approximately 80 percent of the final desired temperature and rises throughout the run. This is due to the energy in the flow that is expended to heat the diaphragm area hardware components upstream of the nozzle throat.

To correlate flight conditions to the supply conditions, the freestream values of pressure and temperature are shown in Figures 10b, 11b and 12b. Pressure and temperature are normalized by ambient conditions at a given altitude for each design point. Notice that the pressure reaches a desired ambient value within approximately 0.5 sec from tunnel start and remains relatively constant during the run due to the operation of the control valves. However, the temperature in the test section rises more slowly, reaching 90 percent of the desired ambient temperature early in the run (0.75 to 2 sec), followed by a gradual rise to 100 percent of the desired value by the end of the run. We define a usable test time to be where the freestream temperature is greater than 90 percent of the desired value. Table 11 lists the nominal supply conditions and achieved freestream pressure and temperature for each rake calibration run.

Inviscid Core Definition

The size and quality of the inviscid core is determined from the following three pieces of information: temporal variations of uniformity, spatial variations of uniformity, and core size as a function of axial position in the test section.

Temporal uniformity is evaluated by plotting Pitot pressure profiles at different snapshots in time. In Figures 13a, 13b and 13c, the calculated local Mach number is normalized by the Mach number calculated from the average of two rake Pitots equidistant (3.5 in.) from the tunnel centerline for each design point. The five times shown are evenly spaced throughout the usable run. Figure 13 shows that the character of the profiles remains unchanged. The temporal variations of each probe measurement are less than the assessed measurement uncertainty. Therefore, no temporal variation can be observed during the usable run time.

Spatial uniformity and core size were determined across the test section for the usable run time. Figures 14 and 15 show Mach number averaged over the entire usable run time for design points 1 and 2 at axial stations of 0.75 in. and 15.75 in.

downstream of the nozzle exit. Pitot measurements were compared with the average of two Pitots, PT13 and PT14 for runs with the rake in the forward station and with PT7 and PT8 for runs with the rake in the aft station. The measured spatial variation in Mach number across the inviscid core is +1.5 to -0.7 percent at the forward rake station and +0.4 to -1.4 percent at the aft rake station for design point 1. The measured spatial variation in Mach number for design point 2 is +1.2 to -0.6 percent at the forward rake station and +1.2 to -1.6 percent at the aft rake station.   Figure 16 shows an average profile at forward rake station for design point 3 with a +1.0 to -1.7 percent spatial variation in the local Mach number. Figures 14-16 also show that for all design points, the core of uniform Mach number is at least 8 in. at the nozzle exit. A consistent feature of the profiles sampled at the nozzle exit is a slight rise in the local Mach number at the tunnel centerline, which corresponds to a drop in the measured Pitot pressure. This is typical of other axisymmetric, hypersonic nozzles including Tunnel 9 nozzles. Calibration data for other Tunnel 9 nozzles can be found in references 11,12 and 13. Spatial variations in all other calculated tunnel conditions based on the local Pitot measurement are listed in Appendix A. Appendix A contains tabular and graphical normalized tunnel conditions for the five rake calibration runs.

From Figures 14 and 15 and an assumption of a linear core convergence between the forward and aft profiles, a uniform inviscid core can be defined. This is shown in Figure 17. For practical planning purposes, the useful inviscid core size is 8 in. in diameter at the nozzle exit and converges axially following a cone half-angle of approximately 4.7 deg. Note that this angle is defined by two measurements, using a Pitot rake with probe spacing of 0.5 in., for design points 1 and 2. The inviscid core will be slightly larger at the higher pressure condition, design point 3, due to a thinner boundary layer along the nozzle wall.

CONE MODEL RESULTS

The second phase of the calibration consisted of a series of runs made at design points 1 and 2 with the blunt cone model. Runs were made with the small and full cone configuration on- and off-centerline, to verify that a uniform aerothermal flowfield existed over the body (on-centerline) or on one side of a representative interceptor forecone configuration (off-centerline). This latter capability would allow the testing of larger model configurations that would not normally fit in the core flow. Definition of the useful cone flowfield was determined from the comparisons of off- and on-centerline pressure and heat transfer data.

Cone Model Pressure Data

Cone pressure data for design points 1 and 2 are shown in Figures 18 through 23. All pressure data are shown in the form of the nondimensional pressure coefficient, Cp,

versus the axial distance from the nose tip. Each figure represents an approximate 1-sec average of each gage during the good flow period of that run.

Figure 18 shows the small cone on-centerline at a design point 1 running condition from Run 2508. The data show a uniform pressure on the cone surface with a small but noticeable difference between the 0-90 deg rays and the 180 and 270 deg rays. This difference was accounted for by a measurable yaw angle misalignment up to 0.25 deg in the cone/sting support structure assembly. This misalignment was discovered and corrected for all subsequent runs but needs to be accounted for in the interpretation of Run 2508 data.

Figure 19 shows Run 2509 cone pressure data made at the design point 2 conditions with the full cone on-centerline. It can be seen that the edge of the uniform core flowfield symmetrically intersects the cone aft of axial instrumentation station 6 at 10 in. from the model nose. This is expected as the aft portion of the cone is outside the usable core boundary and the pressure decreases in this region. Ahead of this boundary, all rays show identical pressure profiles within the reported measurement uncertainty.

Figures 20 and 21 show the 2.5-in. off-centerline pressure data for design points 1 (Run 2512) and 2 (Run 2511), respectively. Both of the runs show the drop in pressure of the bottom and side rays where the cone extends outside of the uniform nozzle core. However, the data taken on the top of the cone (Rays A, B, and C) are nearly identical to the data taken with the cone on-centerline. A comparison with the data from Runs 2508 and 2509 is shown in Figures 22 and 23. Only the last station of Ray C shows a significantly lower pressure signifying this gauge is outside the uniform nozzle core flow for the 2.5-in. off-centerline runs.

A noticeable feature in Figures 22 and 23 is the drop in pressure at stations 4 and 5 (axial location, $x = 6$ and 8 in.) followed by a rise in pressure at station 6 (axial location, $x = 10$ in.) along Ray A for the off-centerline runs. This phenomenon is most noticeable in the design point 2 pressure data shown in Figure 23. This pressure variation along this one ray is real and is a result of the freestream flowfield pressure drop along the tunnel centerline highlighted in the Pitot pressure data discussed above. This pressure drop is axisymmetric within the nozzle and produces a small pressure wave disturbance that can be seen in the shadowgraph flow-visualization photos taken during Runs 2498 and 2511 shown in Figures 24 (a) and (b). Figure 24(a) shows a pressure wave in the freestream during the tunnel start-up of Run 2498. During tunnel start-up the freestream temperatures are low and thus the densities are much higher, making density gradients in the shadowgraph more obvious. During Run 2511, the upper boundary of this disturbance intersects the shock layer and the surface of the cone between instrumentation stations 5 and 6 ($x = 9$ in.). This location coincides with the break-line between the fore and aft cone sections. This interaction produced a weak shock that produced a small higher-pressure region aft of this location. This is

detected by the output of gage PA6, which measured a 17 percent higher pressure than the other gauges at station 6 (PB6 and PC6). However, the effect was spatially small and very localized, damping out prior to station 7 (x = 12 in.) on Ray A and with no measured effect to the B and C rays at either station 6 or 7.

The low pressure region along the tunnel centerline also accounts for the 5 to 10 percent difference between the two runs at station 2 (x = 2 in.) shown in Figure 23. Run 2509 was made with the cone on-centerline, and the pressure instrumentation at stations 1 and 2 are affected by the variation in the freestream pressure. This results in a lower measured pressure at station 2 during Run 2509 than was measured during Run 2511 where the nose tip is mounted outside the centerline pressure drop.

In summary, the pressure data show that a similar uniform flowfield within estimated experimental uncertainty is produced on the top surface of the cone off-centerline as compared to centerline operation. There is no evidence of any radial pressure variations associated with cross-flow along the surface of the cone. Therefore, the pressure data support the hypothesis that the same flowfield can be generated on one side of a configuration that is larger than the core flow by offsetting it relative to the nozzle centerline.

Cone Model Heat Transfer Data

The heat transfer data are compared, in a manner similar to that used for the pressure data, for the same group of runs. All heat transfer data are shown in the form of the nondimensional Stanton number, St, versus the axial distance from the nose tip. All heat transfer figures include, for comparison, representative laminar and turbulent predictions from a boundary-layer integral code from Reference 14.

The first comparison is between Run 2508 and 2509 both centerline runs made at design points 1 and 2, respectively. Figure 25 (Run 2508) shows that instrumentation rays A, D, E and F measured elevated/transitional heat transfer at station 2 (x = 2 in.) and fully turbulent levels aft of station 2, while rays G and H measure laminar levels. This phenomenon is a result of temperature instrumentation coincident with pressure taps along the same ray. The temperature gauges in rays A, D, E and F were mounted 1.75 in. behind the previous tap and 0.25 in. ahead of the tap at the same station to reduce the effect of any surface disturbance on the measurement. However, these small disturbances proved enough to trip the boundary layer. For the G and H rays, where there were no pressure taps, the heating levels remained laminar. The same trend is also present in Run 2509 as shown in Figure 26; however, due to the higher pressure and Reynolds number associated with design point 2, the flow streamlines along rays G and H transitioned naturally aft of station 2 (x = 2 in.) to fully turbulent levels between stations 3 and 5 (x= 4 to 8). Excluding rays G and H, the centerline

data show a uniform profile on all sides of the of the cone that agrees well with predicted turbulent levels.

Figure 27 shows Run 2510, the full cone off-centerline at design point 1. The only variations between Run 2508 and 2510 were the movement of the cone off tunnel centerline and the addition of the aft skirt to the cone for Run 2510. It can be seen that the heat transfer profiles are nearly identical. With the exception of the E ray, which is outside the core in Run 2510, all rays between Runs 2508 and 2510 agree within reported experimental uncertainty as shown in Figure 28. The only exception concerns the natural transition along rays G and H during Run 2510. No transition is seen during Run 2508 with the short cone along rays G and H, but with the addition of the aft skirt section, the full cone provides the additional running length necessary for the development of transition. The transition front also moves forward of station 5 during Run 2510. This onset of a transition and its upstream movement onto the small cone section was not unexpected with the addition of the aft section.

In order to provide consistent boundary-layer transition data and fully turbulent conditions, a boundary-layer trip was added during Runs 2511 and 2512. The trip was constructed of two 0.005-in. OD tungsten-rhenium wires tack-welded to the model surface 0.125 in. downstream of pressure tap station 1 ($x = 0.4$ in.). The trip was necessary to ensure fully turbulent heat transfer levels everywhere on the cone. Schedule and cost constraints prevented the repetition of the previous centerline runs. Therefore, the comparison of the results is not straightforward. Figures 29 and 30 show where the axial Stanton number profiles are affected by the intersection of the core boundary with the model surface mounted off-centerline. Those temperature gauges that were outside the inviscid core showed a dramatic drop in the measured temperature, resulting in a much lower calculated Stanton number. The station at which the Stanton number deviates from the turbulent levels defines the region where the uniform nozzle core intersects the surface.

A comparison is also made between the on- and off-centerline heat transfer levels to evaluate any effect due to only part of the cone being in the inviscid core. Figures 31 and 32 show design points 1 and 2 on- and off-centerline comparisons. In each case, the turbulent level centerline data come from rays A, D, E, and F and are compared to rays A, F and G on the top surface of the cone mounted off-centerline. Figure 31 shows good agreement with the exception of station 2 because of the transitional nature of the station 2 data from Run 2508 as described above. Figure 32 shows excellent agreement within the experimental uncertainty between the two design point 2 runs. Figures 31 and 32 both show some small effect of the variation in tunnel freestream pressure conditions along the tunnel centerline as was discussed in the previous section. Ray A during Runs 2511 and 2512 shows a dip of 5 percent in the calculated Stanton number that corresponds with the drop in pressure that was observed. This variation still remains within the experimental uncertainty for Stanton

number, and is not considered a significant variation for aerothermal and thermal structural testing.

<u>Cone Data Conclusions</u>

Combining the results of both the pressure and heat transfer instrumentation, a region is defined where uniform full-flight conditions are produced on one side of the sphere-cone model positioned off-centerline. Figure 33 shows a graphical representation of the cone surface highlighting the area that remains within the inviscid core that defines the usable wetted surface area. This useful area is representative of the size and position available to test full-scale interceptor seeker windows.

TUNNEL CONDITIONS

The supply and test cell tunnel conditions are determined by the achieved heater conditions and the inner diameter/open area of the ablator seat. Three ablator seats were manufactured and tested corresponding to the three design points. After the rake runs and prior to the cone runs, the design point 2 ablator seat was modified. The inner diameter was opened approximately 0.01 in. to prevent overstressing of the main restrictor body. This change in open area had a small effect on the achieved supply pressure for the same nominal heater pressure. P_0 increased from approximately 5500 psia to approximately 6000 psia resulting in an increase in freestream pressure from 1.5 to 1.6 psia. This increase in pressure adjusted the altitude of duplication of design point 2 from approximately 16 km closer to the desired 15 km. Future tunnel runs at the calibration design point 2 will closely resemble cone runs 2509 and 2511.

Table 2 lists the nominal expected test conditions and the associated altitude duplication. Nominal supply pressure will vary slightly, on the order of 100 psi, from run to run. Other run conditions can be achieved with the manufacture of new ablator seat hardware as well as from the variation of supply pressure and temperature. The facility currently duplicates the thermal structural environment at Mach 7 for altitudes down to 11.5 km and up to 20 km. It has the potential to produce environments as low as 10 km and as high as 25 km. Higher Reynolds number operation could also be achieved by operating at lower supply temperatures, producing a Mach number / Reynolds number simulation without a true temperature altitude match.

During future testing it may not be practical or possible to make a Pitot measurement in the test cell freestream without interfering with the test model. One option is to use a model stagnation pressure tap. Otherwise, a method for calculating freestream conditions is necessary. An experimental correlation of the Pitot pressure was developed based on measured supply and Pitot pressures from all of the calibration rake runs. This correlation was determined from the average of the rake

Pitot probes located 3.5 in. from the tunnel centerline and is valid only during the good flow portion of a run using the Mach 7 nozzle for supply temperatures 2700 °F < T_0 < 3000 °F. This linear relation is shown in Figure 34. The remaining freestream conditions are calculated using this Pitot pressure and the measured supply pressure and temperature as described in a previous section.

SUMMARY

The Tunnel 9 Thermal Structural Facility has undergone calibration. Operation at three design points has been verified. The facility produces freestream pressures and temperatures that will duplicate flight at altitudes between 38,000 and 67,000 ft (11.5 - 20.5 km) at Mach 7 (6560 ft/s or 2 km/s) for up to 5 sec of run time. The facility has demonstrated an 8-in. inviscid core at the nozzle exit uniform to within +1.5 to -1.7 percent of Mach number at all conditions. The validity of testing on one side of a model configuration that is larger than the core by positioning it off-centerline has been demonstrated. In conclusion, the Tunnel 9 Thermal Structural Facility has been completed and is ready to support flight duplication thermal structural testing in support of interceptor programs.
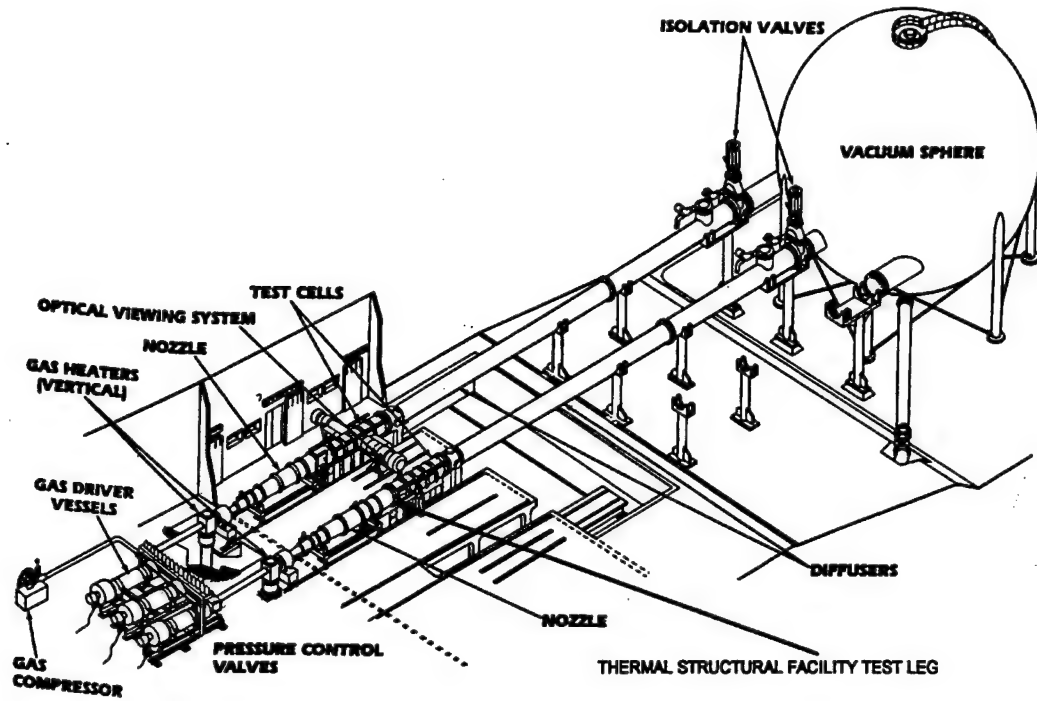
FIGURE 1. HYPERVELOCITY WIND TUNNEL NO. 9
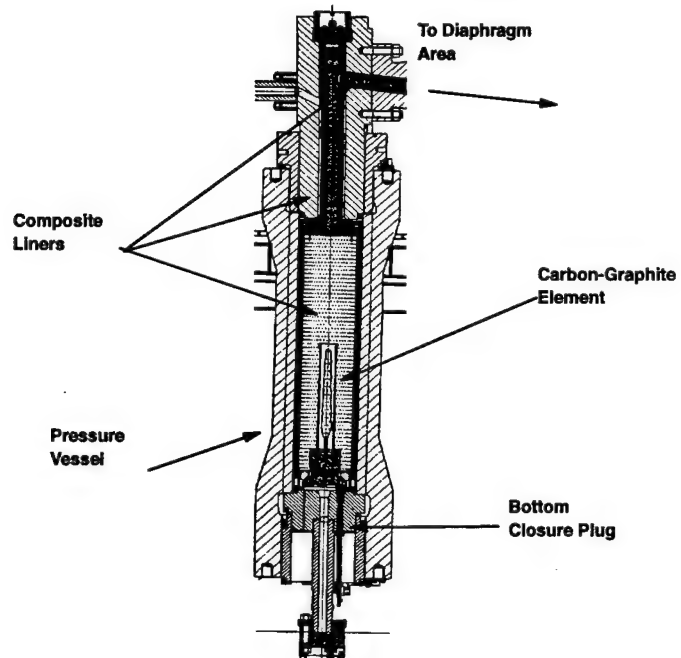
FIGURE 2. CENTER LEG HIGH TEMPERATURE SUPPLY HEATER
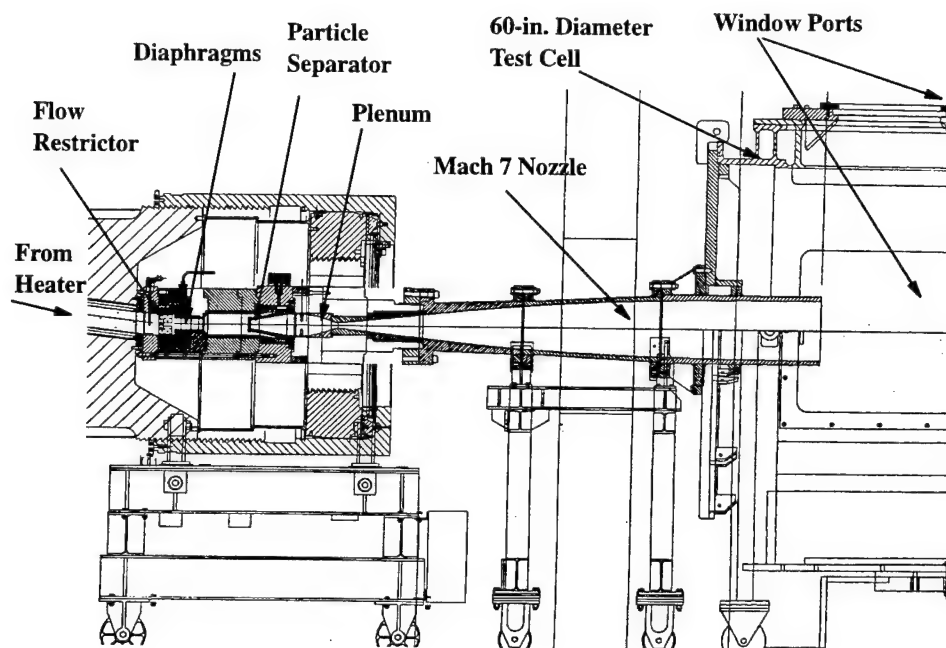
FIGURE 3. MACH 7 DIAPHRAGM AREA AND NOZZLE
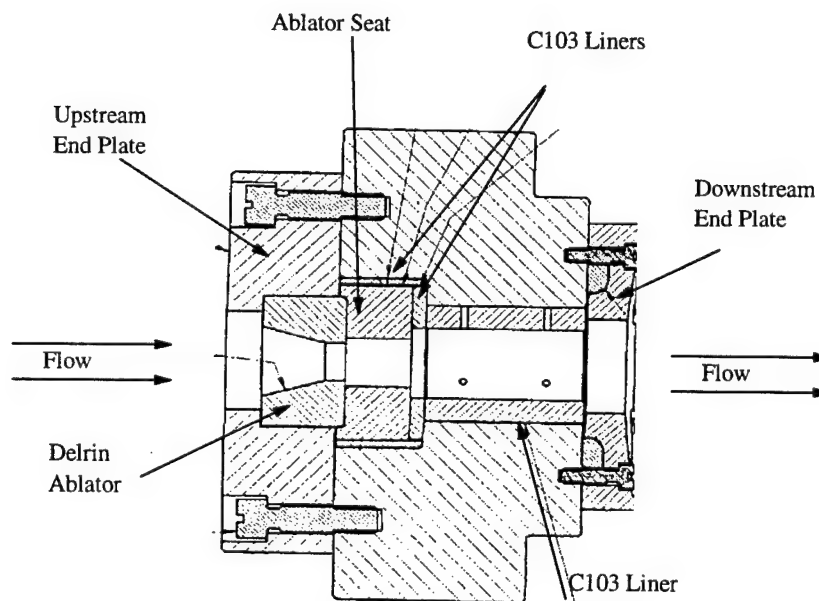
FIGURE 4. FLOW RESTRICTOR ASSEMBLY
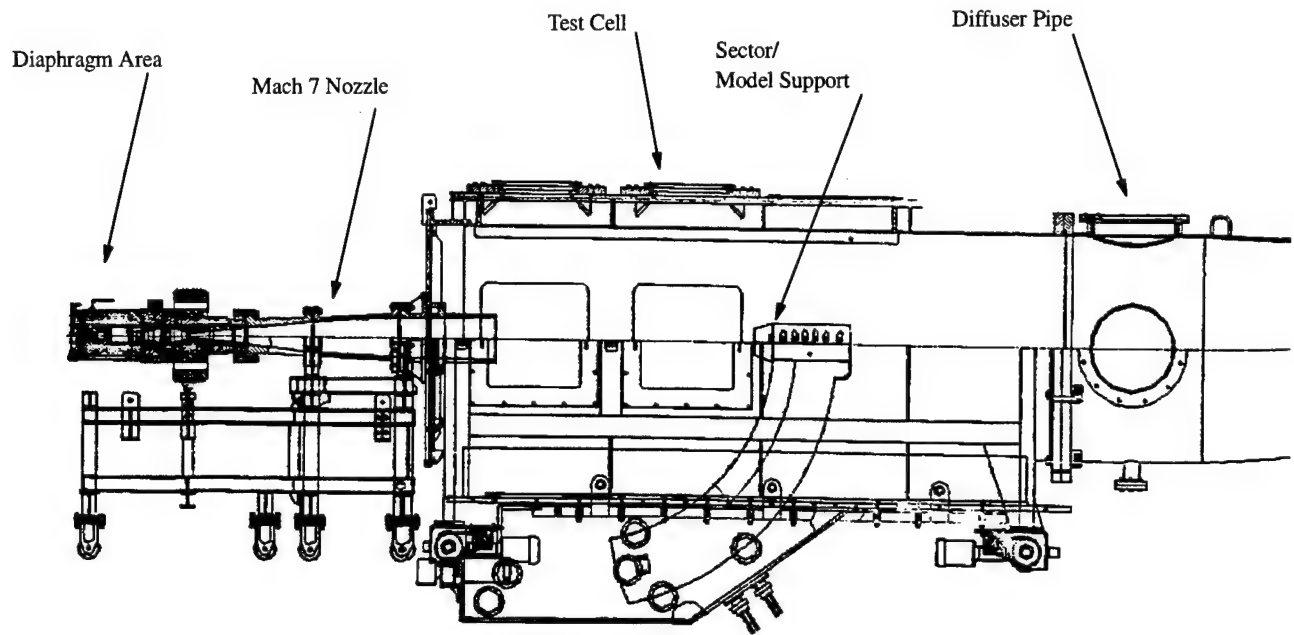
FIGURE 5. THERMAL STRUCTURAL FACILITY NOZZLE AND TEST CELL SCHEMATIC
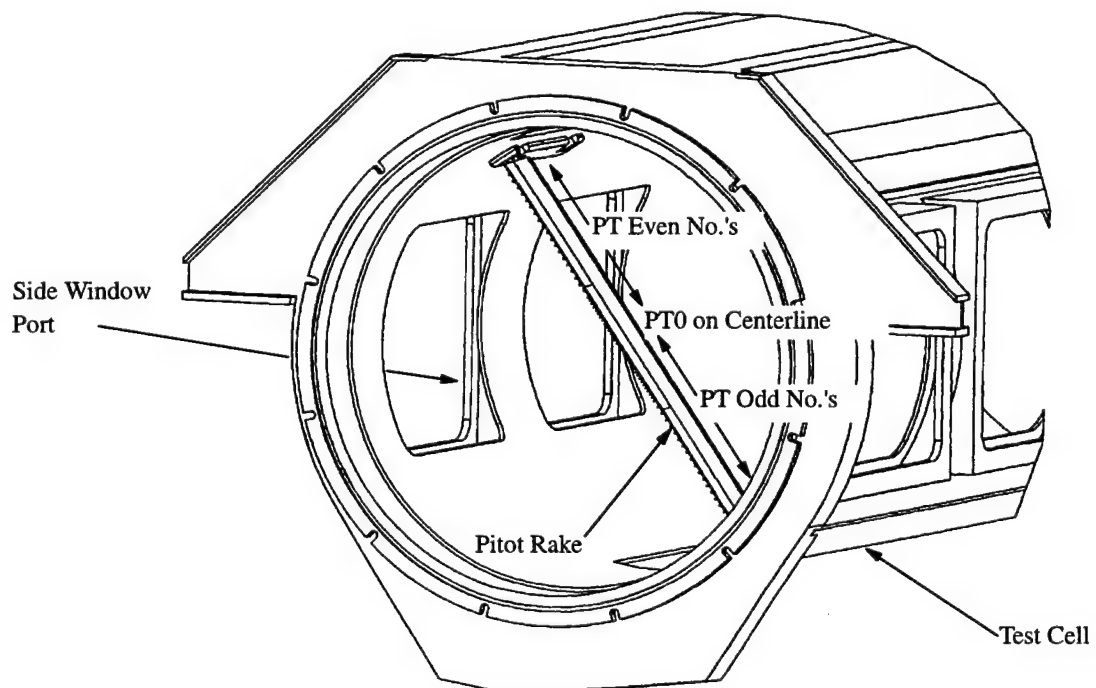
FIGURE 6. WALL MOUNTED PITOT RAKE SETUP AND NOMENCLATURE

Tantalum Pitot Tube

O-Ring

Air Cooling Line

Columbium C-103
Leading Edge

Kulite XT-140-200a
Pressure Transducer
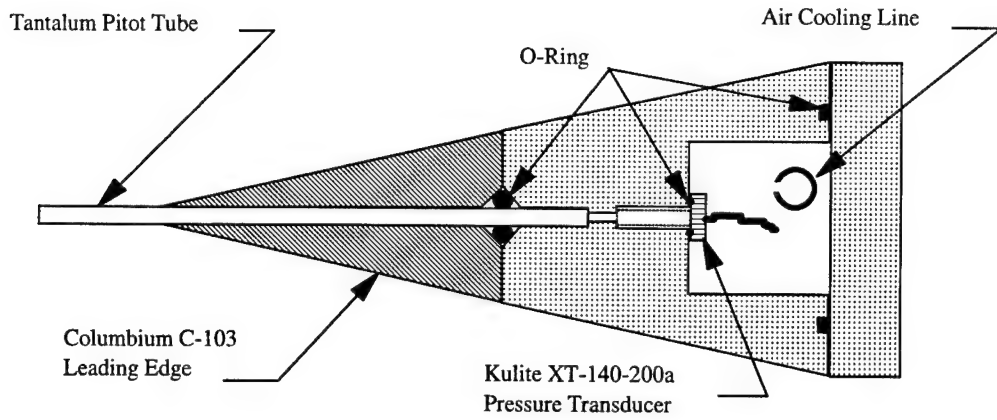
FIGURE 7. CALIBRATION RAKE CROSS-SECTIONAL VIEW

MACH 7
CENTER LEG

0 1 2 3 4 5 6 7 8 9 10

GRAPHIC SCALE = FEET
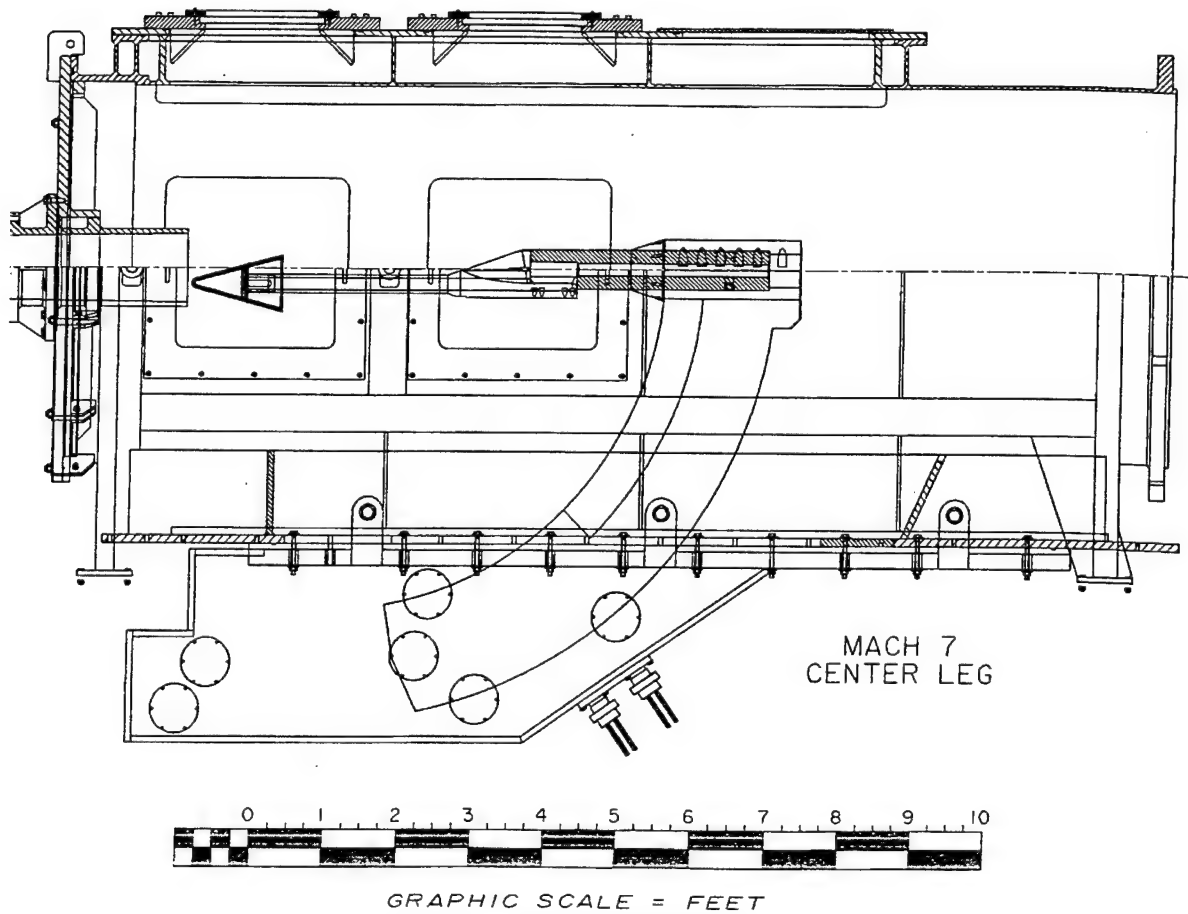
FIGURE 8. SPHERE CONE/STING/TEST CELL ASSEMBLY, WITH CONE 2.5 IN.
BELOW CENTERLINE

24
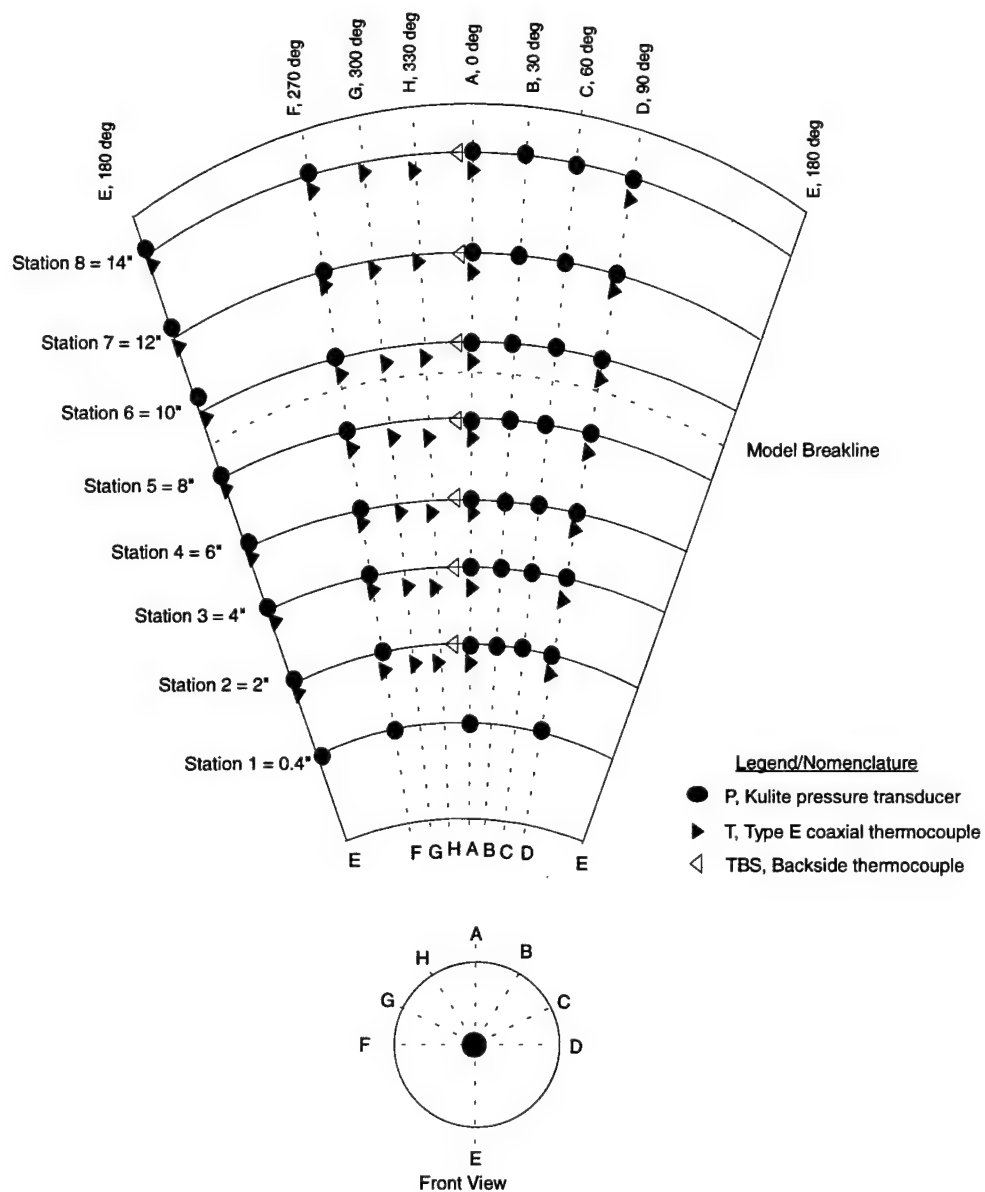
FIGURE 9. CONE MODEL INSTRUMENTATION LAYOUT

Run 2498 (67 kft)
Measured Tunnel Conditions
□ P0   ◇ T0   ○ Pitot

(A). MEASURED CONDITIONS

Run 2498 (67 kft)
Test Cell Freestream
□ Pinf / Pamb (67 kft)   ◇ Tinf / Tamb (67 kft)

1962 Std. Atmosphere
Pamb = 0.75 psia
Tamb = 389.97 degR
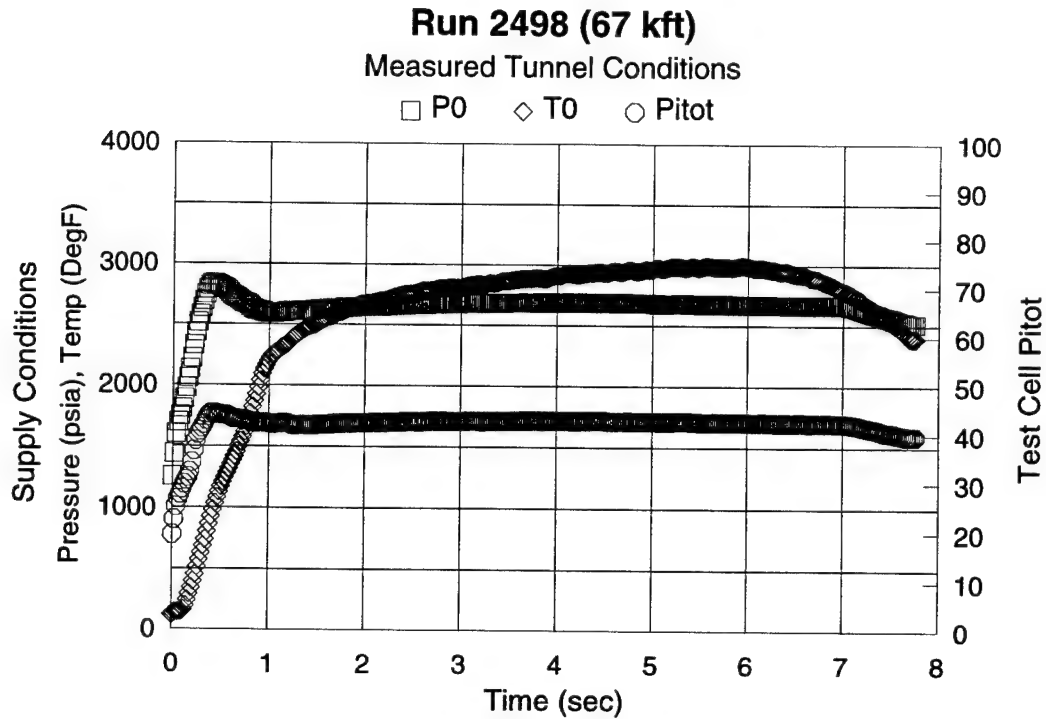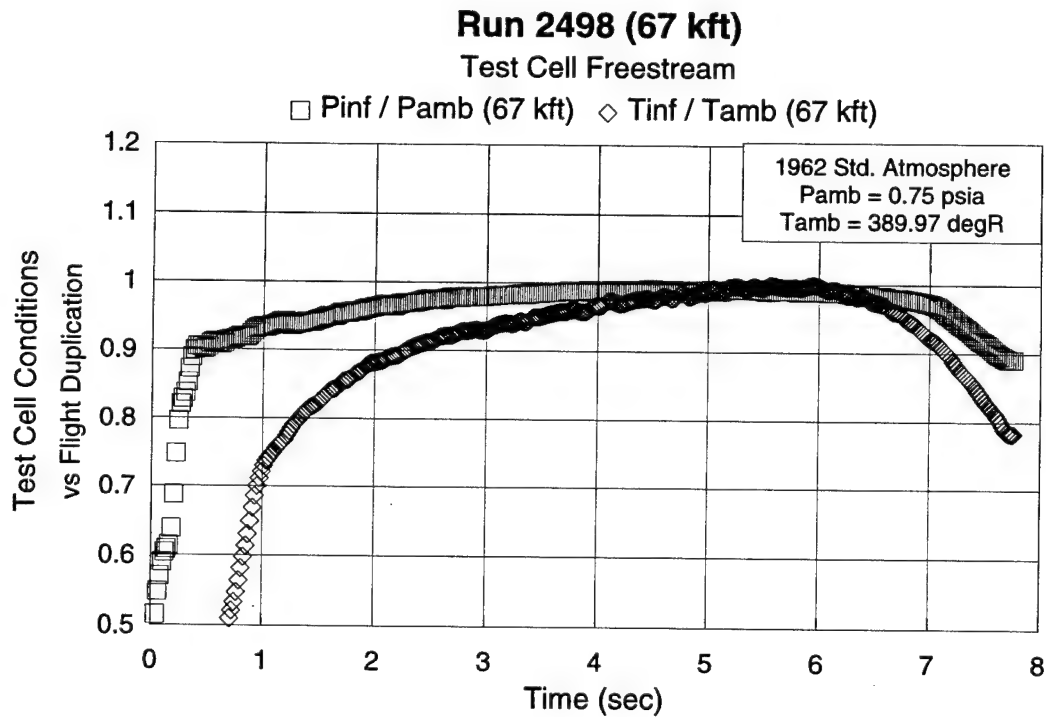
(B). FREESTREAM VS AMBIENT AT ALTITUDE

FIGURE 10. DESIGN POINT 1 ACHIEVED CONDITIONS

Run 2496 (52.5 kft)

Measured Tunnel Conditions

□ P0   ◇ T0   ○ Pitot
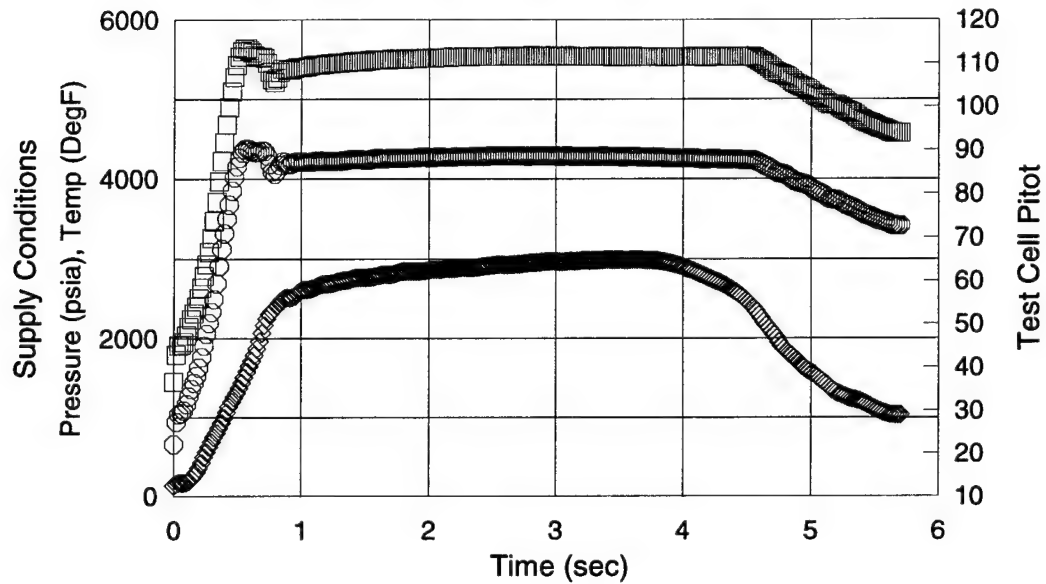
(A). MEASURED CONDITIONS

Run 2496 (52.5 kft)

Test Cell Freestream

□ Pinf / Pamb (52.5 kft)   ◇ Tinf / Tamb (52.5 kft)

1962 Std. Atmosphere
Pamb = 1.5 psia
Tamb = 389.97 degR
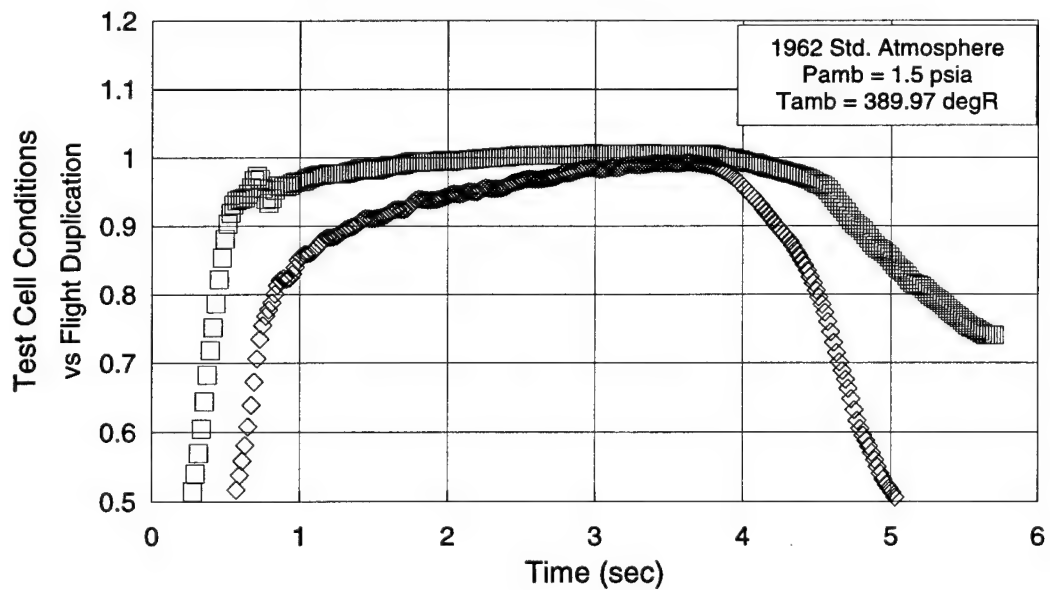
(B). FREESTREAM VS AMBIENT AT ALTITUDE

FIGURE 11. DESIGN POINT 2 ACHIEVED CONDITIONS

Run 2506 (38 kft)

Measured Tunnel Conditions

□ Po   ◇ To   ○ Pitot

(A). MEASURED CONDITIONS

Run 2506 (38 kft)

Test Cell Freestream

□ Pinf / Pamb (38 kft)   ◇ Tinf / Tamb (38 kft)

1962 Std. Atmosphere
Pamb = 3.00 psia
Tamb = 389.97 degR

(B). FREESTREAM VS AMBIENT AT ALTITUDE
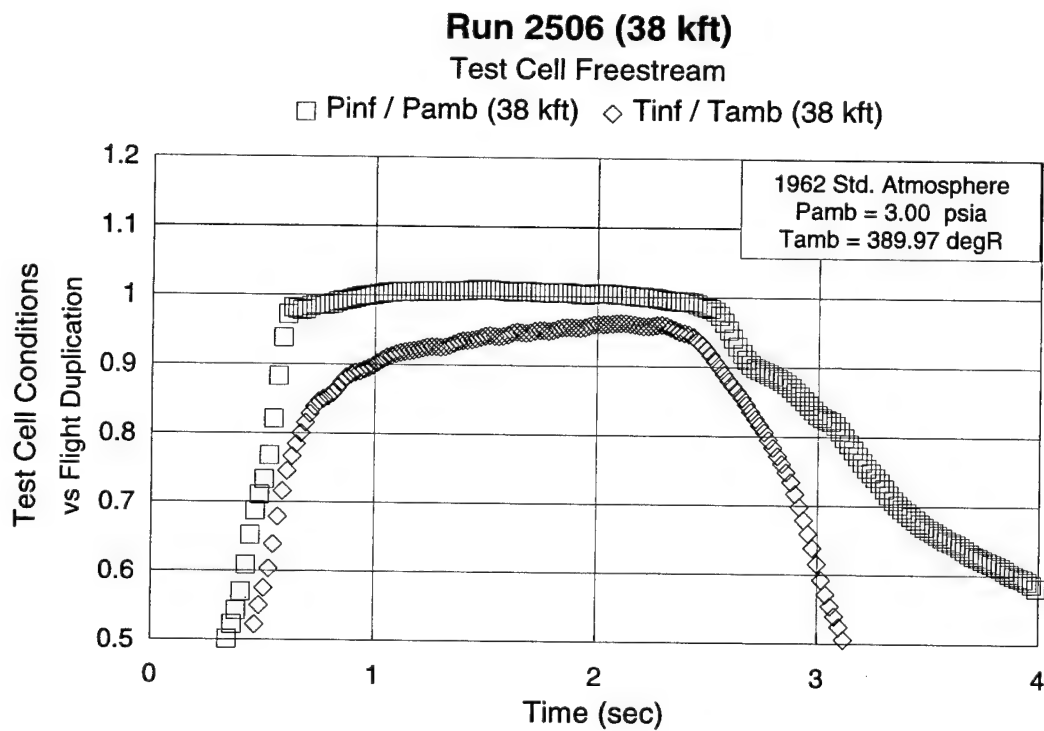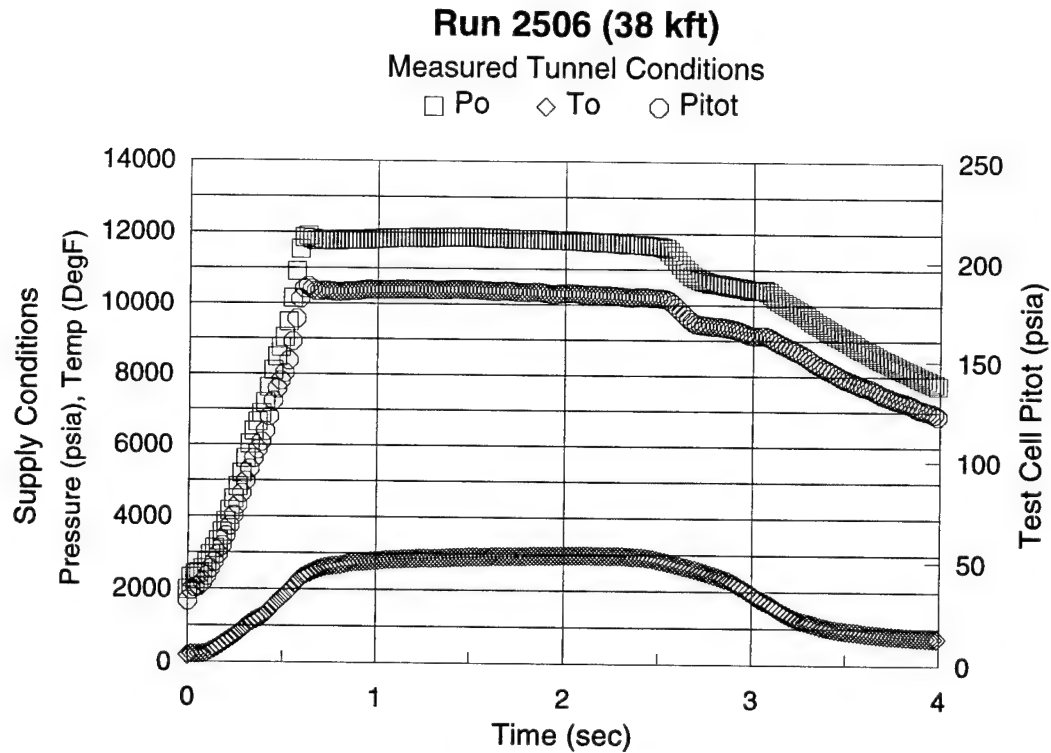
FIGURE 12. DESIGN POINT 3 ACHIEVED CONDITIONS

Run 2493

Temporal Profile Variations of Normalized Mach Number
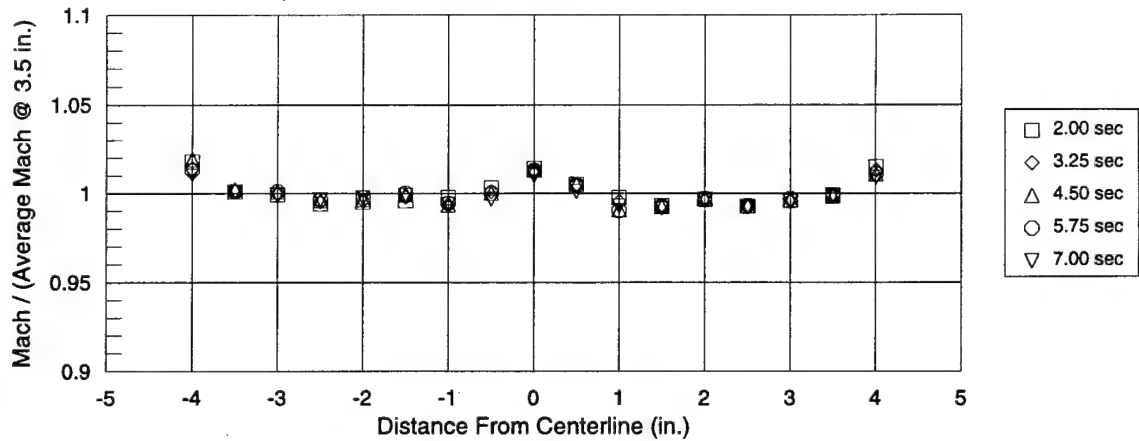
(A). DESIGN POINT 1 / RUN 2493

Run 2496

Temporal Profile Variations of Normalized Mach Number
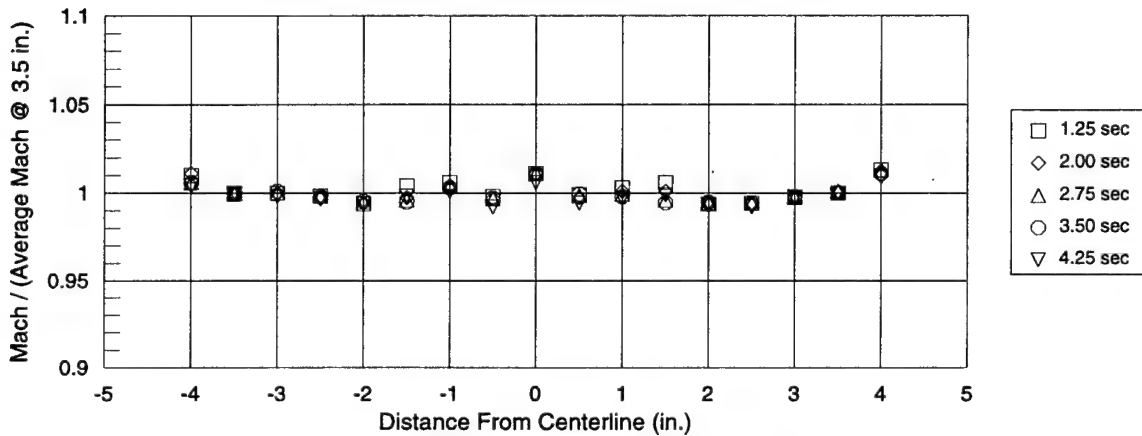
(B). DESIGN POINT 2 / RUN 2496

Run 2506

Temporal Profile Variations of Normalized Mach Number
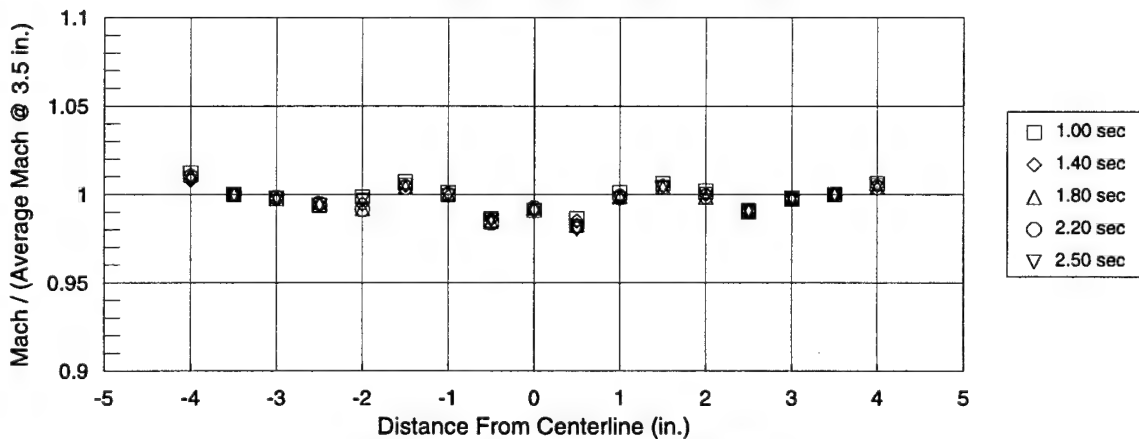
(C). DESIGN POINT 3 / RUN 2506

FIGURE 13. INVISCID CORE PROFILE TEMPORAL VARIATIONS

Run 2493

Average Mach Number Profile (2.0 - 7.0 sec)

(A). FORWARD RAKE LOCATION (X = 0.75 IN.)
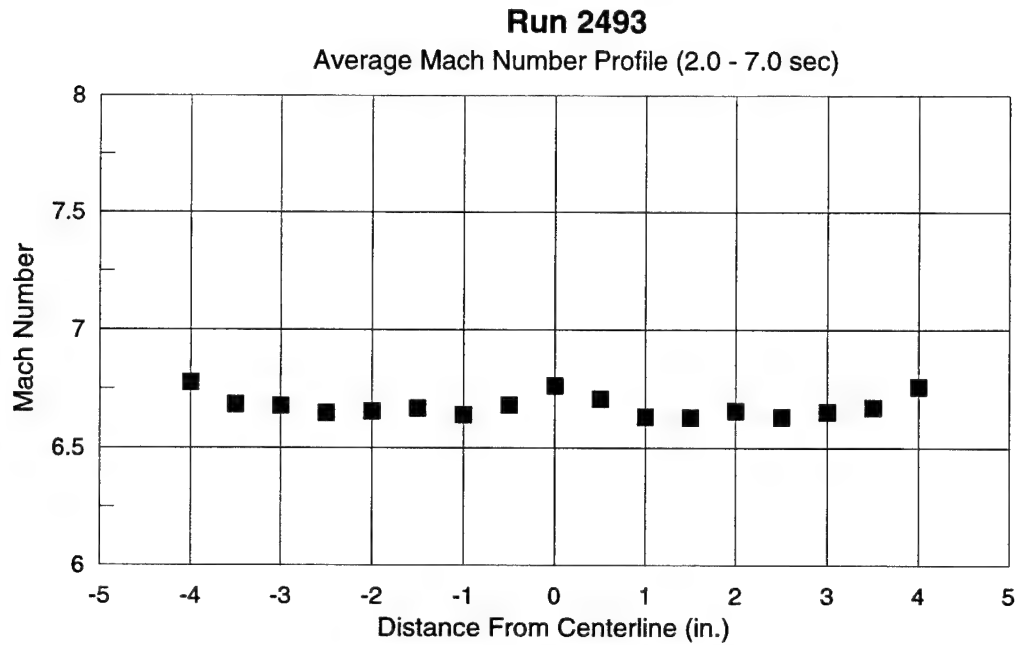
Run 2498

Average Mach Number Profile (2.0 - 7.0 sec)
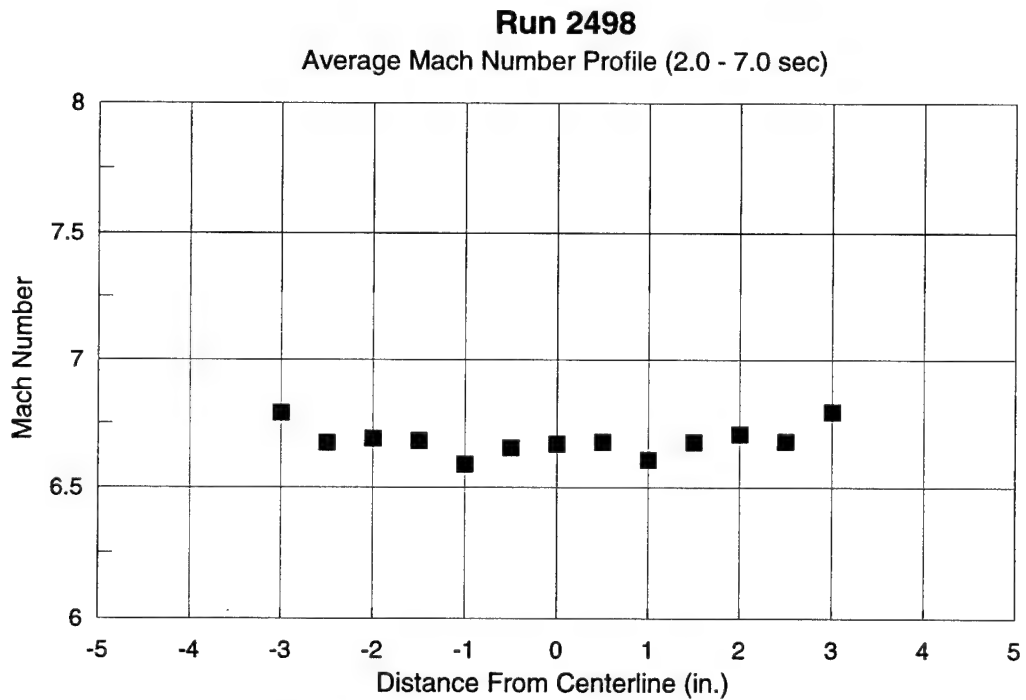
(B). AFT RAKE LOCATION (X = 15.75 IN.)

FIGURE 14. AVERAGE MACH NUMBER PROFILE DESIGN POINT 1

Run 2496

Average Mach Number Profile (1.25 - 4.25 sec)
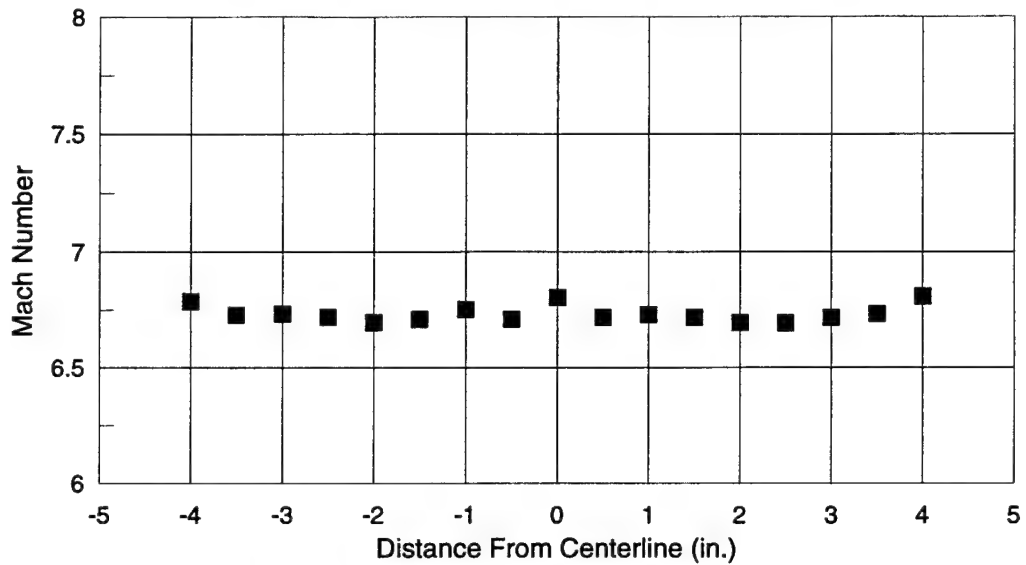
(A). FORWARD RAKE LOCATION (X = 0.75 IN.)

Run 2497

Average Mach Number Profile (1.25 - 4.25 sec)
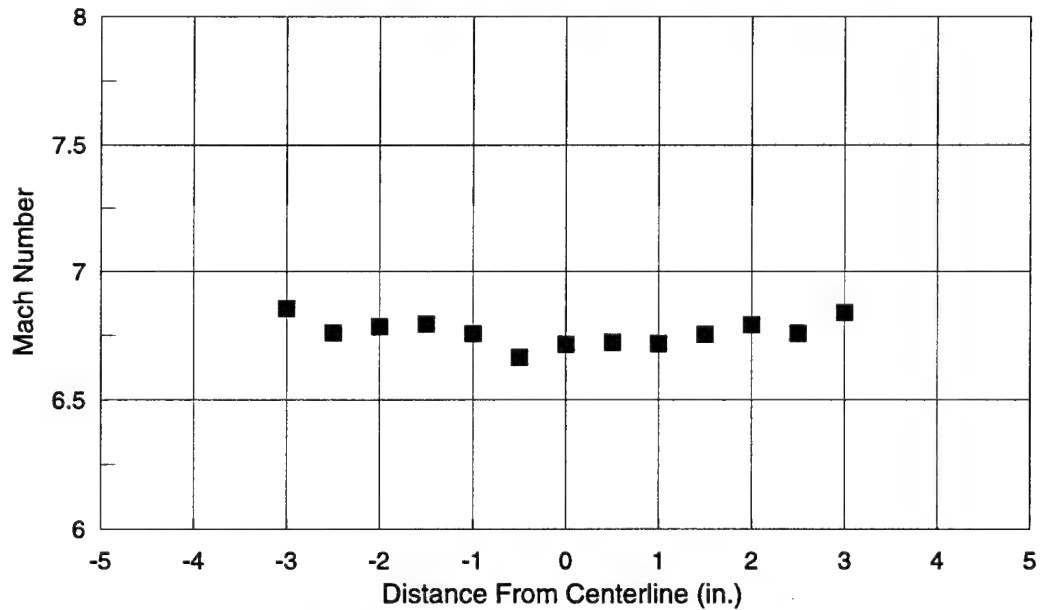
(B). AFT RAKE LOCATION (X = 15.75 IN.)

FIGURE 15. AVERAGE MACH NUMBER PROFILE DESIGN POINT 2

Run 2506

Average Mach Number Profile (1.0 - 2.5 sec)
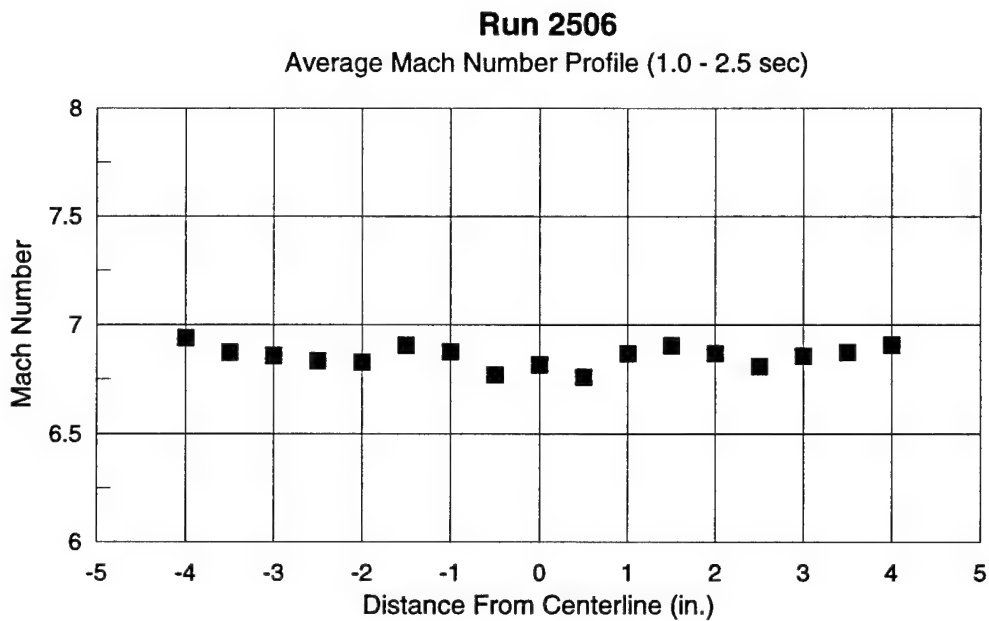
FIGURE 16. AVERAGE MACH NUMBER PROFILE DESIGN POINT 3
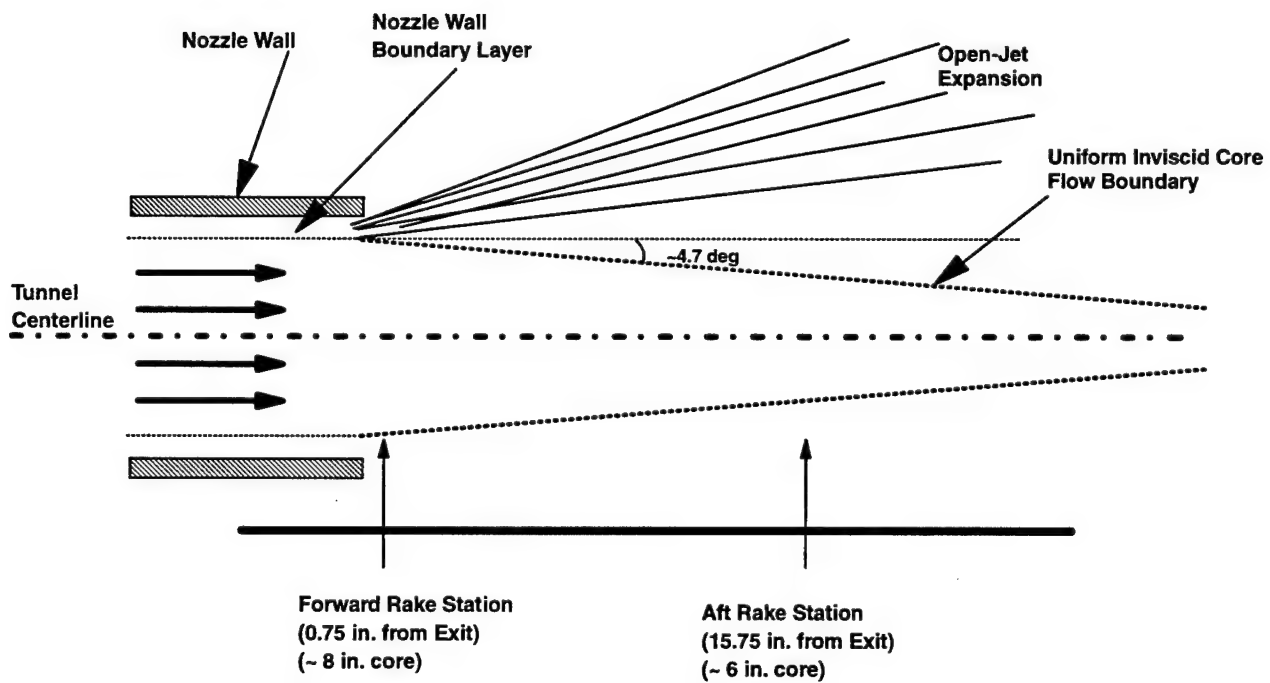
FIGURE 17. AXIAL INVISCID CORE SIZE DEFINITION AT MACH 7
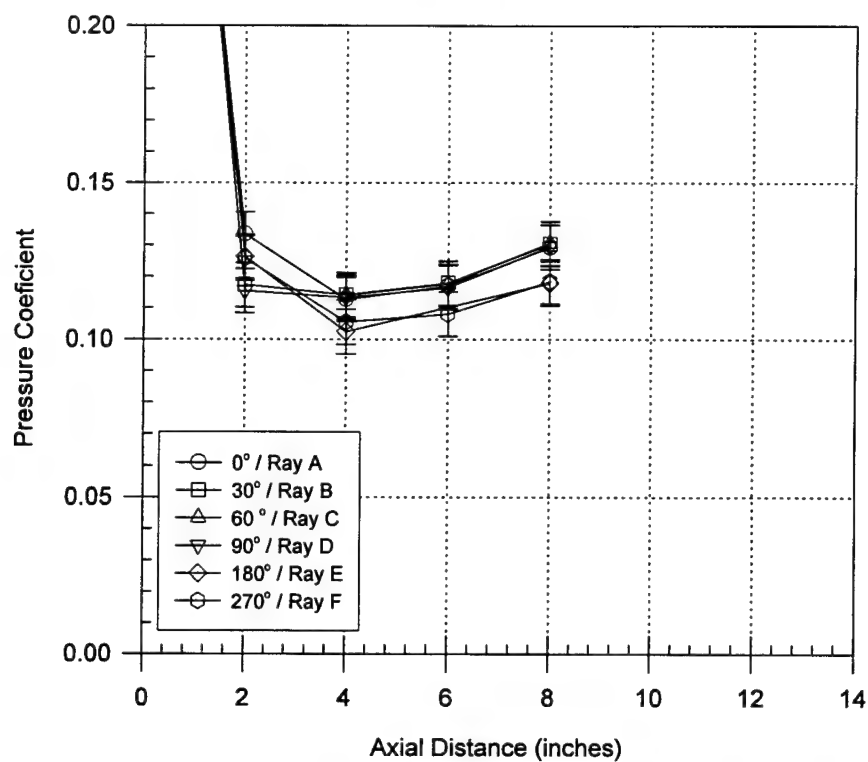
FIGURE 18. PRESSURE COEFFICIENT FOR THE SMALL CONE ON-CENTERLINE, DESIGN POINT 1, RUN 2508
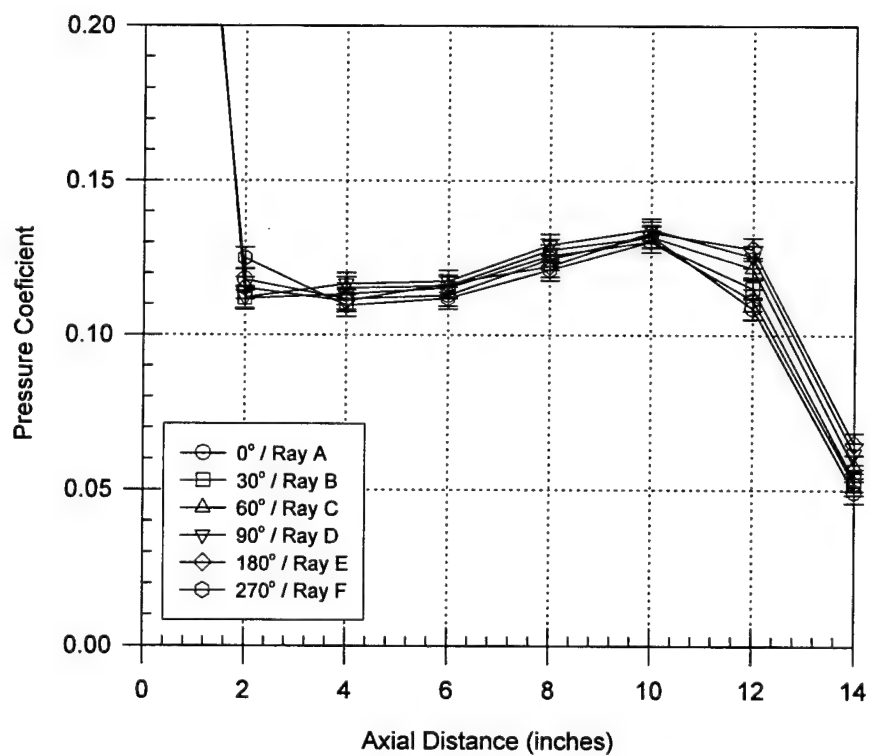
FIGURE 19. PRESSURE COEFFICIENT FOR THE FULL CONE ON-CENTERLINE, DESIGN POINT 2, RUN 2509
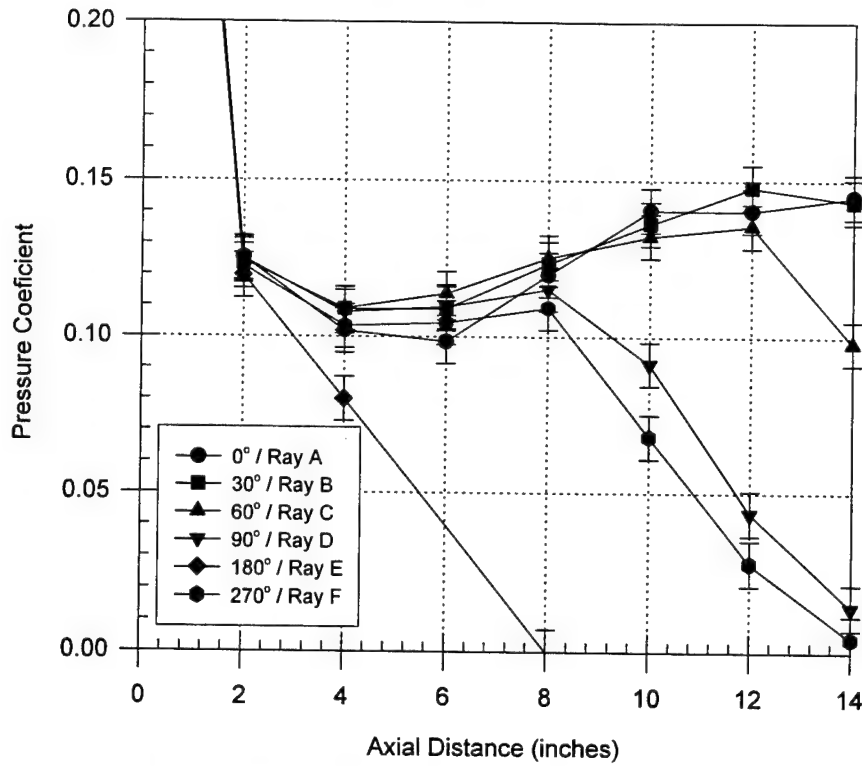
FIGURE 20. PRESSURE COEFFICIENT FOR THE FULL CONE OFF-CENTERLINE,
DESIGN POINT 1, RUN 2512
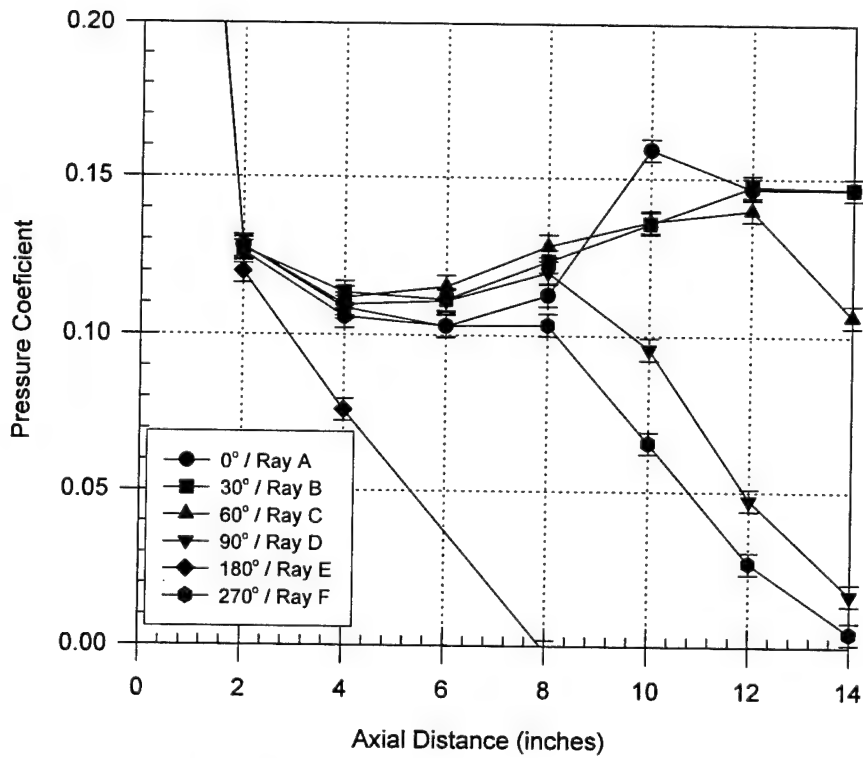
FIGURE 21. PRESSURE COEFFICIENT FOR THE FULL CONE OFF-CENTERLINE,
DESIGN POINT 2, RUN 2511
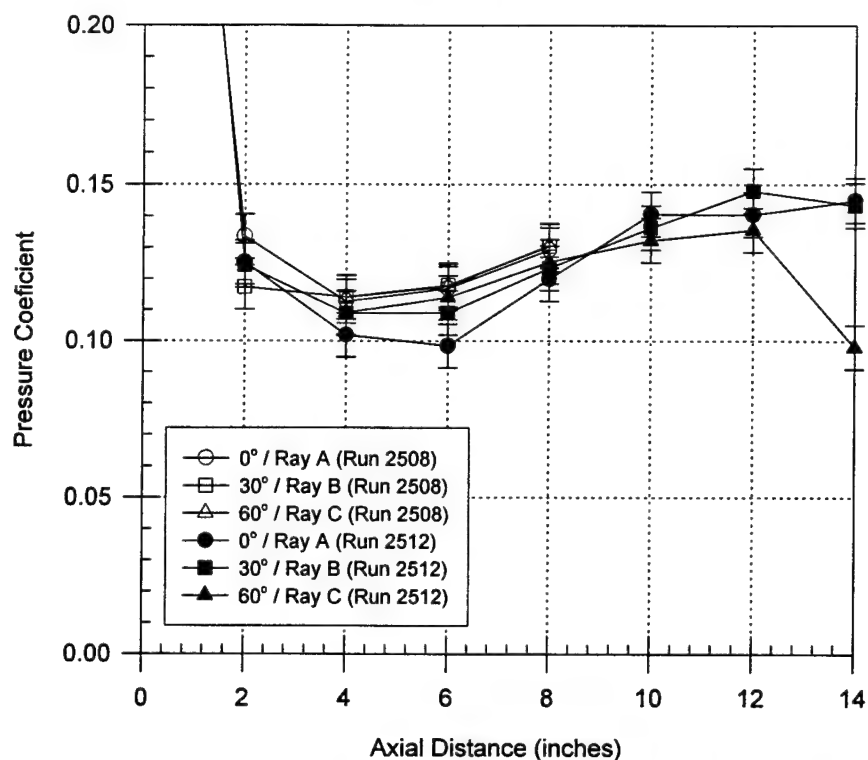
FIGURE 22. COMPARISON OF ON- AND OFF-CENTERLINE PRESSURE COEFFICIENT
FOR DESIGN POINT 1
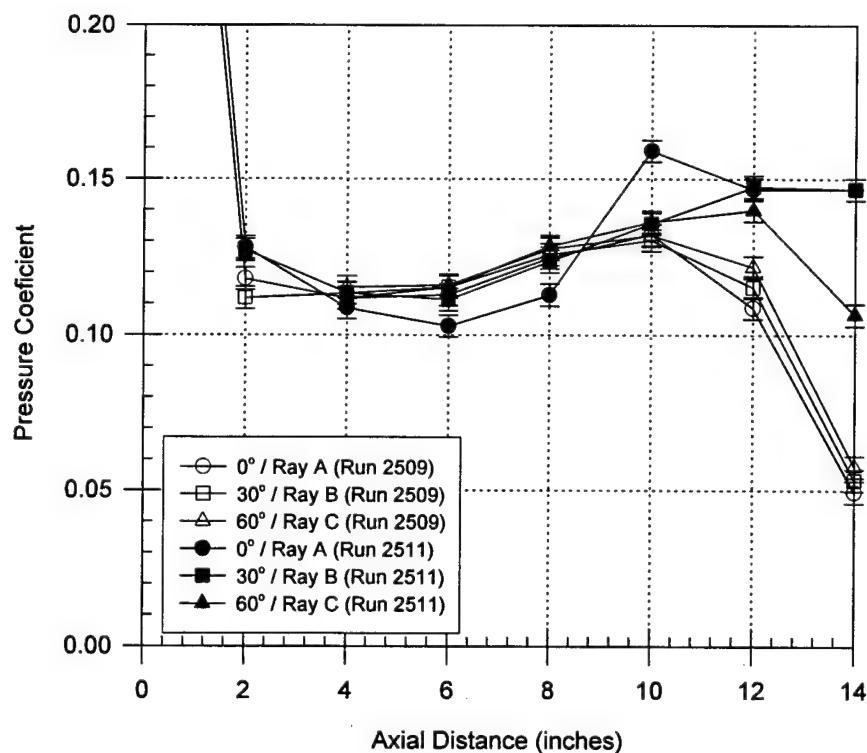
FIGURE 23. COMPARISON OF ON- AND OFF-CENTERLINE PRESSURE COEFFICIENT
FOR DESIGN POINT 2
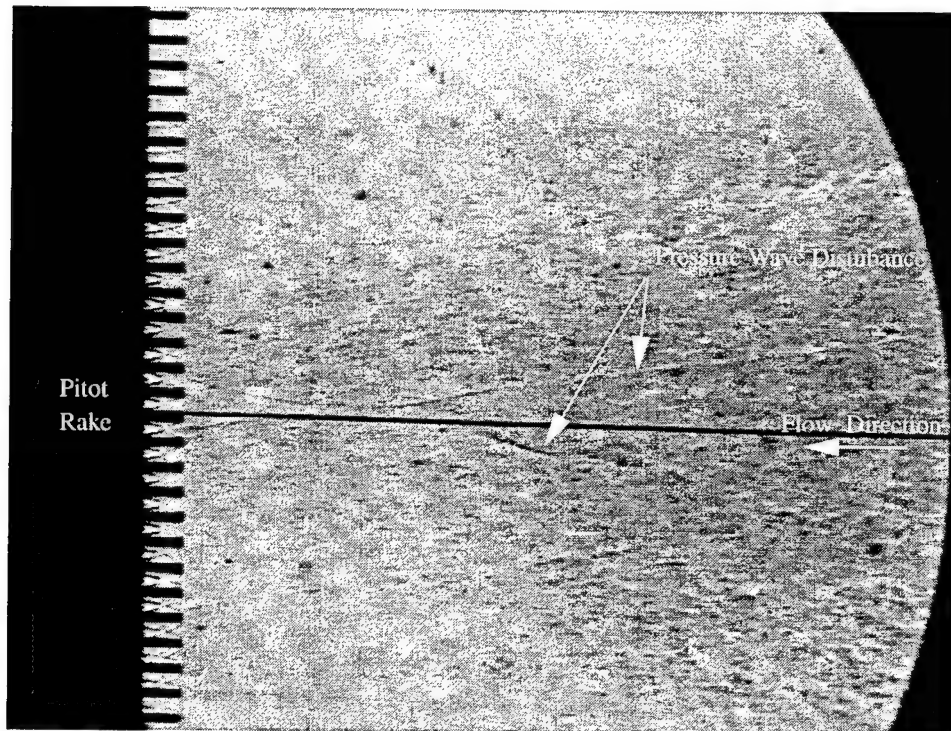
FIGURE 24(A). SHADOWGRAPH DURING TUNNEL START-UP, DESIGN POINT 2, RUN 2498
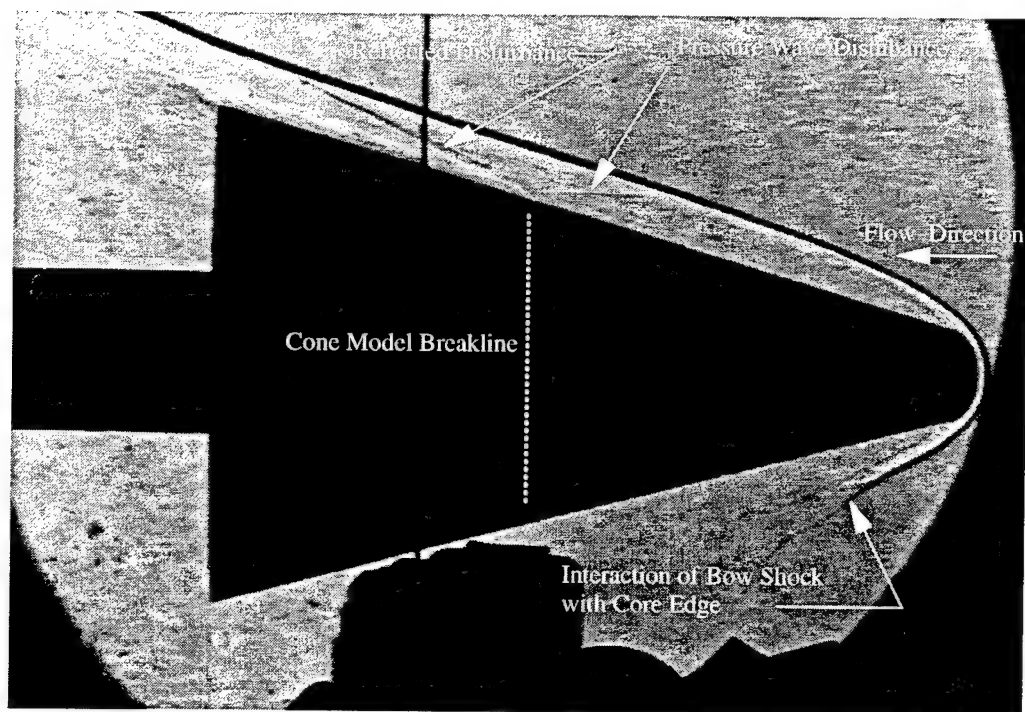
FIGURE 24(B). SHADOWGRAPH OF CONE OFF-CENTERLINE, DESIGN POINT 2, RUN 2511
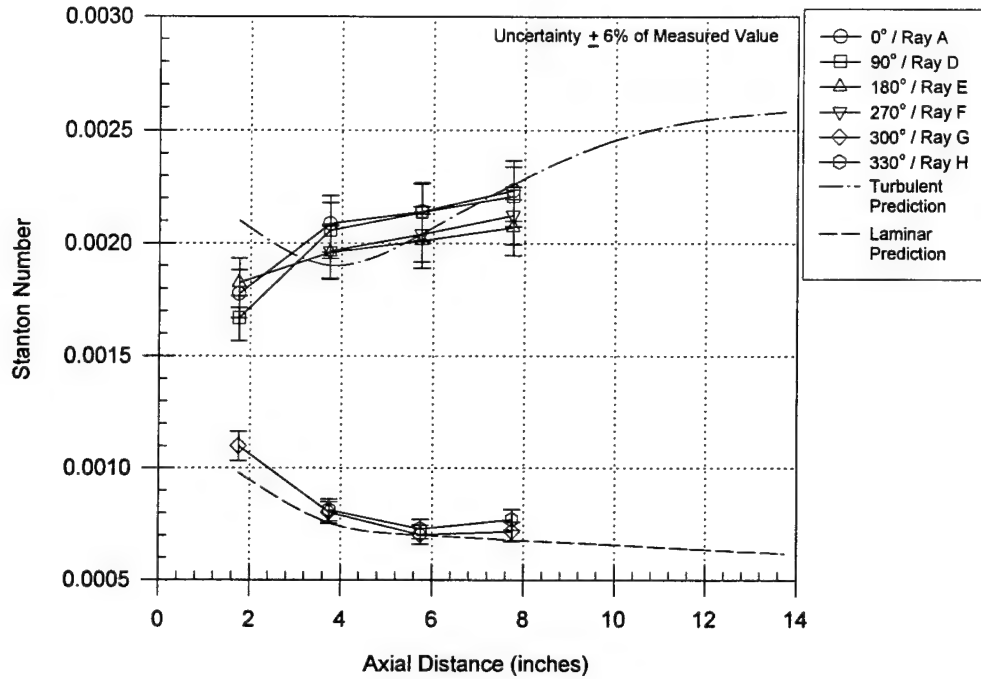
FIGURE 25. STANTON NUMBER FOR THE SMALL CONE ON-CENTERLINE AT DESIGN POINT 1
NO BL TRIP, RUN 2508
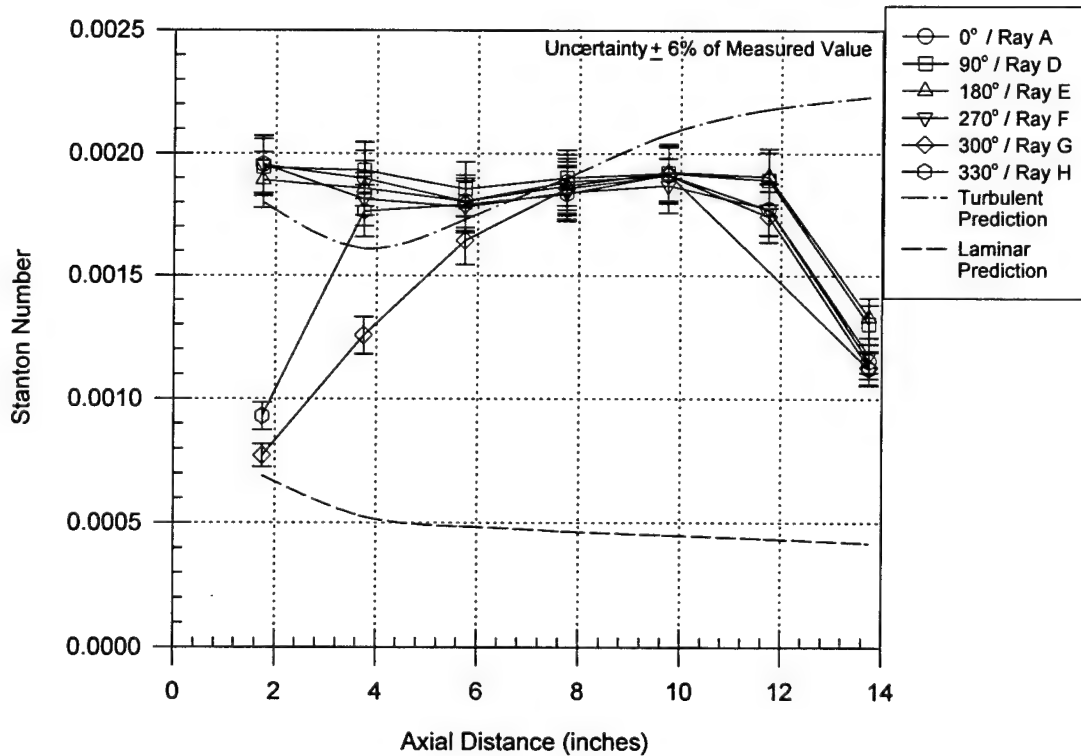
FIGURE 26. STANTON NUMBER FOR THE FULL CONE ON-CENTERLINE AT DESIGN POINT 2,
NO BL TRIP, RUN 2509

37
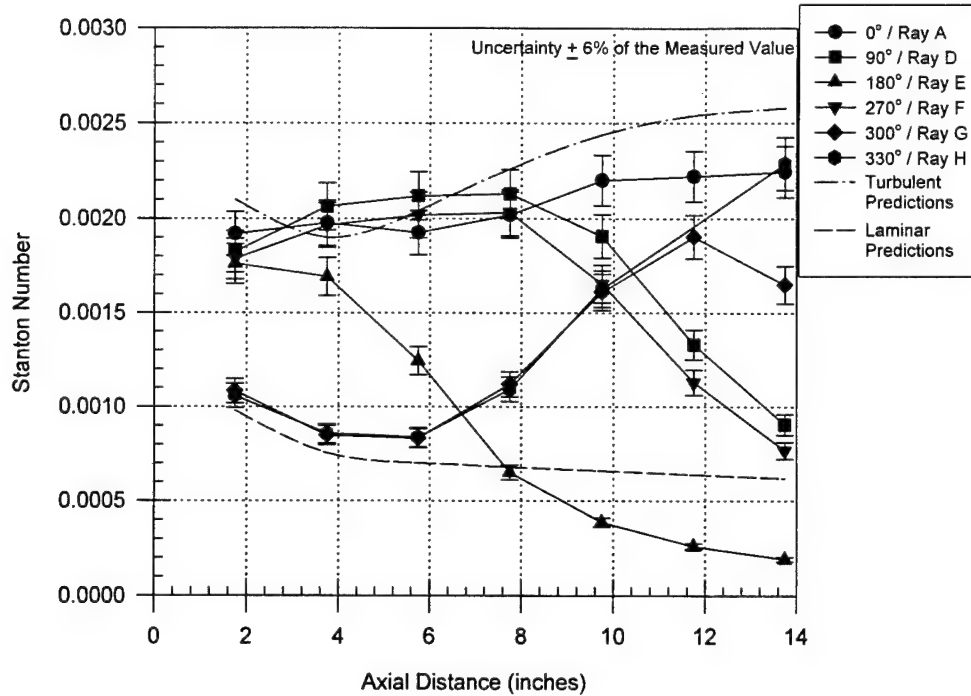
FIGURE 27. STANTON NUMBER FOR THE FULL CONE OFF-CENTERLINE AT DESIGN POINT 1,
NO BL TRIP, RUN 2510
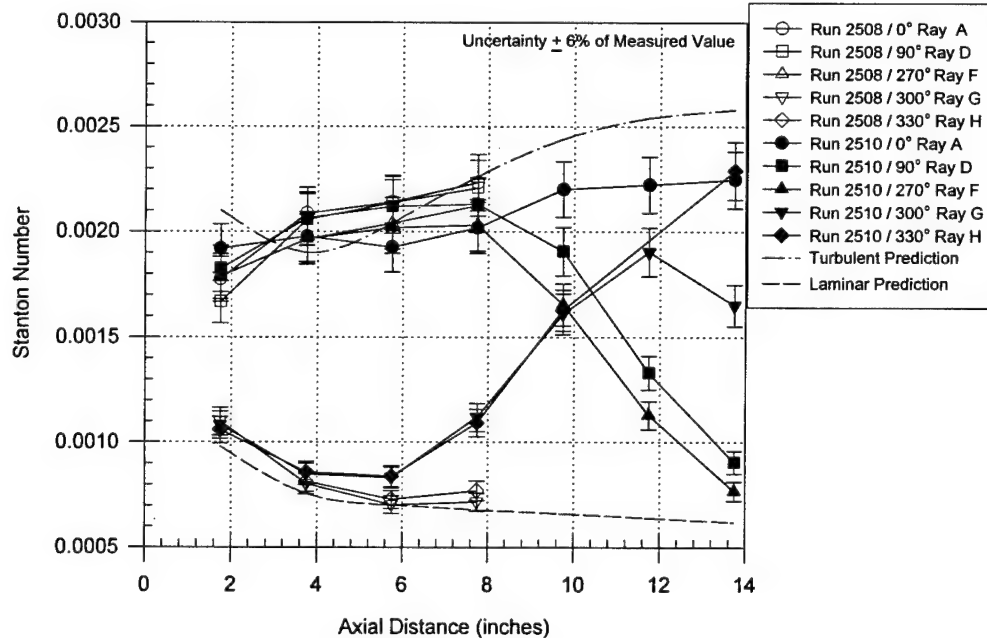
FIGURE 28. COMPARISON OF ON- AND OFF-CENTERLINE STANTON NUMBER
FOR DESIGN POINT 1, NO BL TRIP
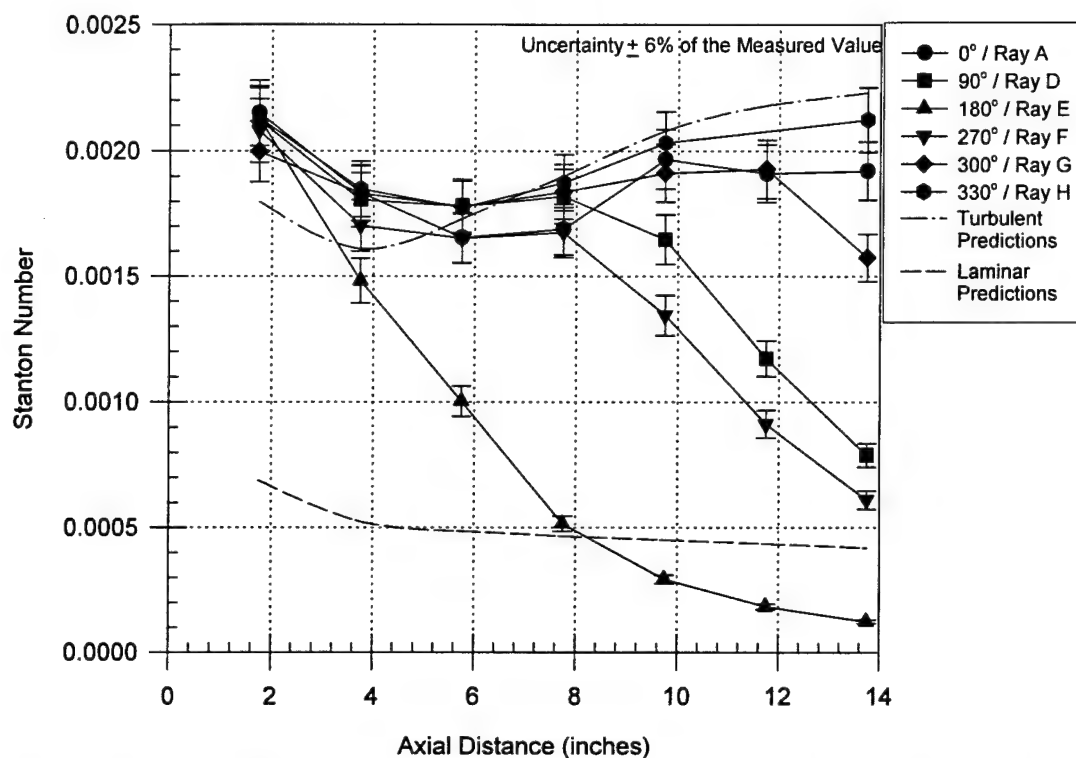
FIGURE 29. STANTON NUMBER FOR THE FULL CONE OFF-CENTERLINE AT DESIGN POINT 2
WITH BL TRIP, RUN 2511
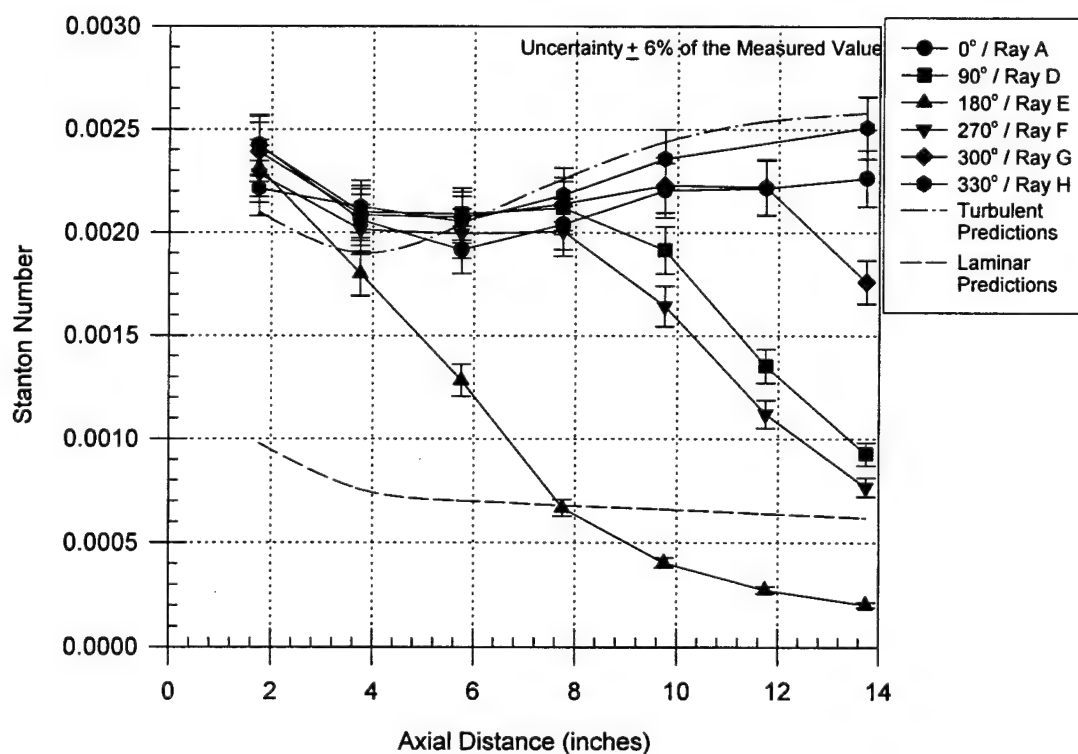
FIGURE 30. STANTON NUMBER FOR THE FULL CONE OFF-CENTERLINE AT DESIGN POINT 1
WITH BL TRIP, RUN 2512

39
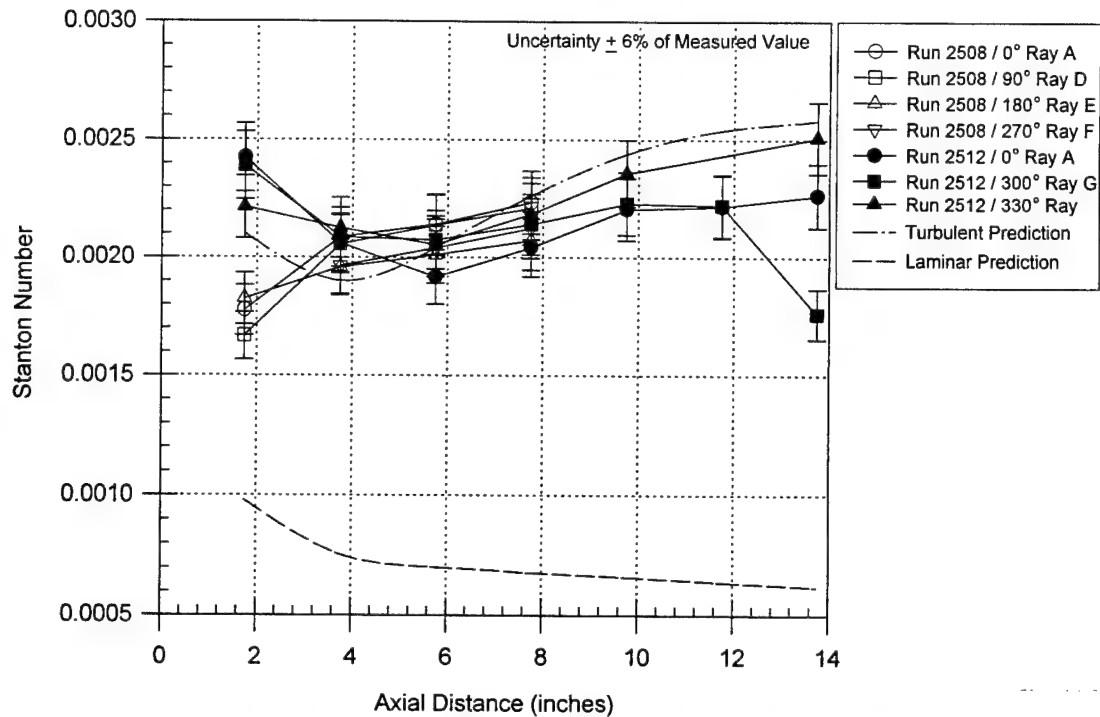
FIGURE 31. COMPARISON OF ON- AND OFF-CENTERLINE STANTON NUMBER FOR DESIGN POINT 1
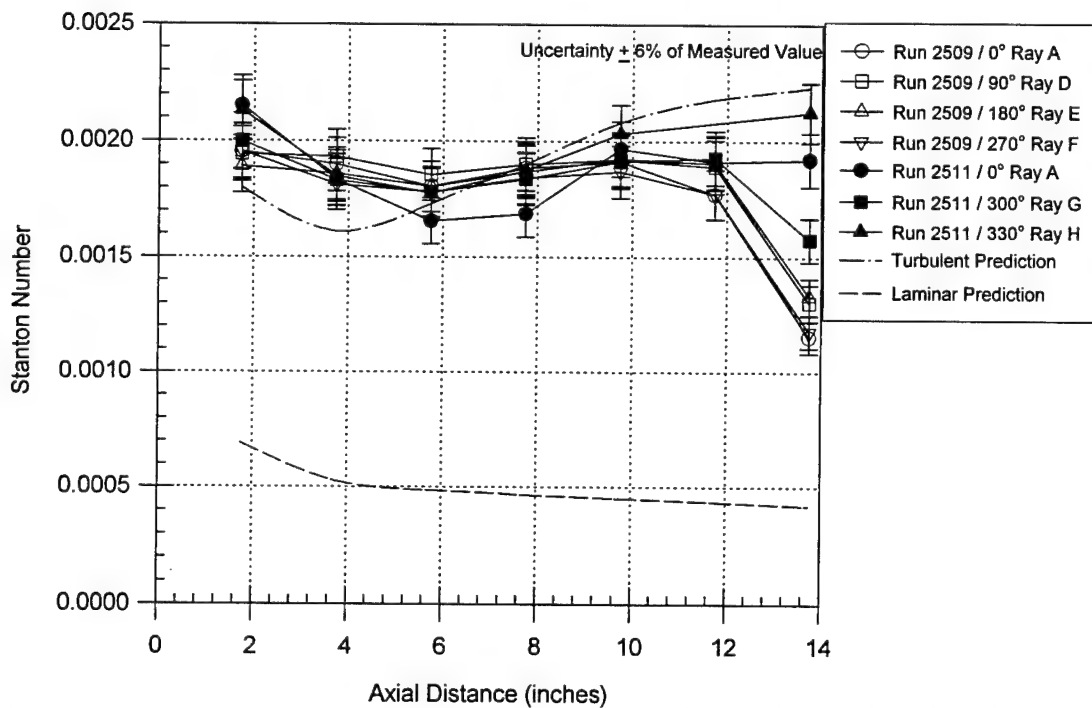
FIGURE 32. COMPARISON OF ON- AND OFF-CENTERLINE STANTON NUMBER FOR DESIGN POINT 2
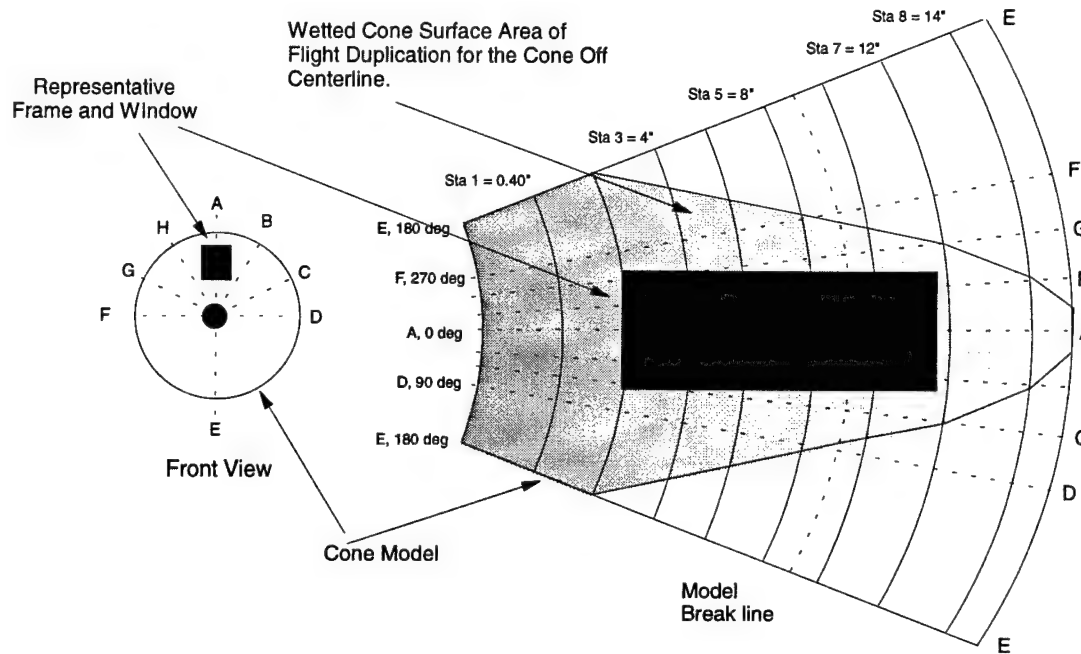
FIGURE 33. USABLE CONE MODEL SURFACE FOR CONE POSITIONED 2.5 IN. BELOW CENTERLINE
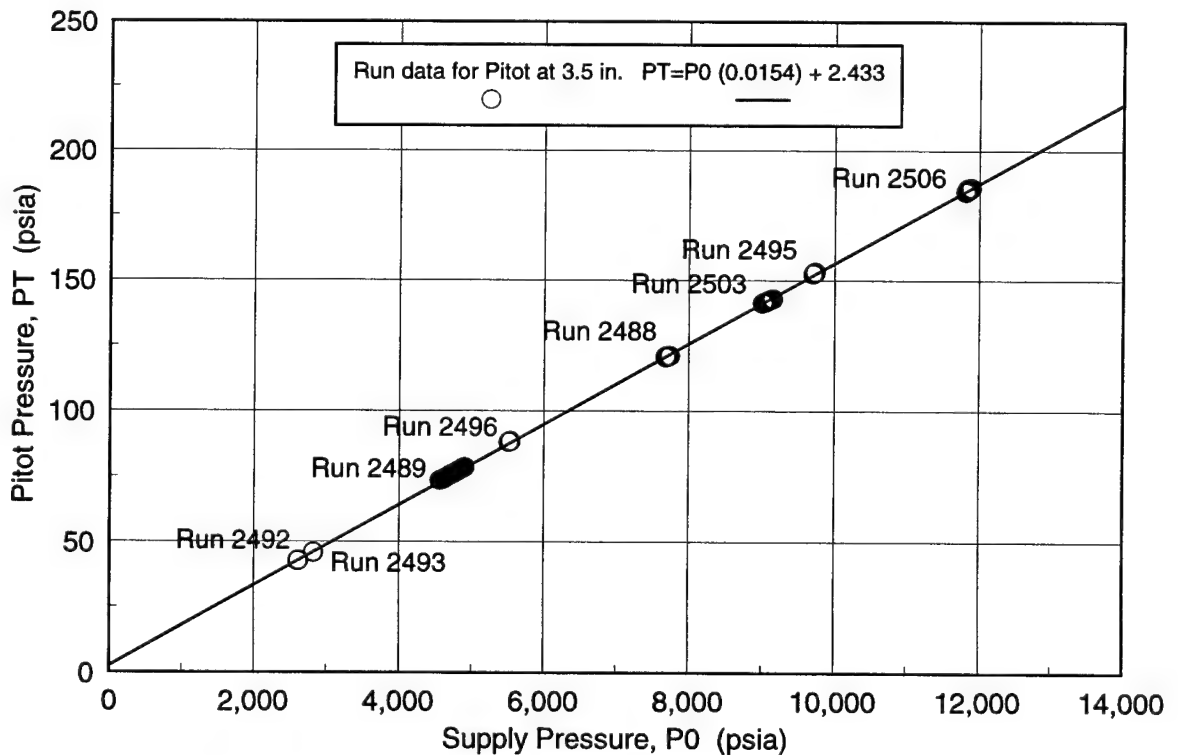
FIGURE 34. MACH 7 PITOT PRESSURE SUPPLY PRESSURE RELATION

41

TABLE 1. NSWCDD HYPERVELOCITY WIND TUNNEL NO. 9 CAPABILITIES

Contoured Nozzle	Reynolds Number Range (million/ft)	Supply Pressure Range (psia)	Nominal Supply Temperature (°F)	Usable Run Time Range (sec)	Comment
7	3.7 - 15.8	2,700 - 12,000	3,000	1.75 - 5	Flight duplication of P and T
8	8.7 - 55.7	2,000 -12,000	1,200	0.2 - 0.75	Flight duplication of dynamic pressure
10	0.86 - 21.9	500 - 14,000	1,350	0.23 - 15	High Reynolds number naturally turbulent boundary layers with pitch capability
14	0.072 - 4.0	100 - 19,000	2,700	0.7 - 15	High Reynolds number/ High Mach number simulation with pitch capability
16.5	2.65 - 3.2	19,000 - 21,000	2,800	3.0 - 3.5	

TABLE 2. REPRESENTATIVE DESIGN CONDITIONS FOR THERMAL STRUCTURAL DUPLICATION BASED ON 1962 STANDARD ATMOSPHERE

Design Point	Duplication Altitude (kft / km)	P_{amb} or P_{inf} (psia / kPa)	T_{amb}/T_{inf} (deg R / °K)	U_{inf} (ft/s / km/s)	Run Time (sec)
1	66 / 20	0.8 / 5.5	389.97 / 216.65	6400 / 1.95	5
2	51 / 15.5	1.6 / 11.0	389.97 / 216.65	6500 / 1.98	3
3	38 / 11.5	3.0 / 20.7	389.97 / 216.65	6600 / 2.01	1.75

TABLE 3. LIST OF INOPERATIVE GAUGES FOR EACH PRIMARY CALIBRATION RUN

Run No./Model	Inoperative Gauges
2493/Rake	none
2496/Rake	none
2497/Rake	none
2498/Rake	none; (P_0 shunt calibration was bad-reduced using shunt cal from 2508)
2506/Rake	none
2507/Small Cone	PC2, TF2, TH2
2508/Small Cone	PC2, TF2, TH2
2509/Full Cone	PC2, PE1, PE4, PF1, TH7, TBS8, BAS3
2510/Full Cone	PC2, PE4, BAS2, BAS3, TBS8
2511/Full Cone	PC2, PE4, BAS3, TBS8
2512/Full Cone	PC2, PE4, TH7, BAS3

TABLE 4. UNCERTAINTY ESTIMATES OF MEASURED TUNNEL CONDITIONS

Measured Quantity (units)	Gauge Type or S/N	Range	Bias (B)	Precision (P)	dof	Uncertainty (U_{rss} ±)
Supply Pressure, P0 (psi)	663777	10000	11.56	2.3	>30	11.79
	665462[1]	20000	63.02	40.03	>30	74.66
	665462[2]	20000	61.83	4.95	>30	61.83
Supply Temperature T0 (°F)	W-5%RE vs W-26%RE	4200	20.86	0.0831	>30	20.86
Pitot Press. (psi) [3]	Kulite XT-140	200	0.140	0.0368	>30	0.145
Pitot Press. (psi) [4]	Kulite XT-140	200	0.307	0.108	>30	0.325
Pitot Press. (psi) [5]	Kulite XT-140	200	0.495	0.075	>30	0.501

1. Recorded on DARE channel 4, runs 2496 and 2497.
2. Recorded on DARE channel 201, runs 2506 and 2507
3. Design Point 1, 20.5 km duplication, runs 2493, 2498, 2508, 2510 and 2512.
4. Design Point 2, 16 km duplication, runs 2496, 2497, 2507, 2509 and 2511.
5. Design Point 3, 11.5 km duplication, run 2506.

TABLE 5. ESTIMATED UNCERTAINTIES OF CALCULATED VALUES FOR DESIGN POINT 1

Parameter units	Nominal value	B	P	U_{rss} ±
Mach	6.697	0.008876	0.001772	0.009051
q_∞ (psia)	24.82	0.07535	0.0198	0.07791
T_∞ (°R)	380.4	3.084	0.1832	3.089
P_∞ (psia)	0.7902	0.003946	0.0009744	0.004064
Re/L (1/ft)	3.86e+06	3.86e+04	2.33e+03	3.87e+04
U_∞ (ft/sec)	6515	21.49	0.2121	21.49
ρ_∞ (lbm/ft^3)	5.42e-03	3.97e-05	4.53e-06	3.99e-05
ρU_∞ (lbm/ft^{2}s)	35.3	0.16	0.02883	0.1625

TABLE 6. ESTIMATED UNCERTAINTIES OF CALCULATED VALUES FOR DESIGN POINT 2

Parameter units	Nominal value	B	P	$U_{rss}\pm$
Mach	6.711	0.01896	0.01172	0.02229
q_∞ (psia)	48.57	0.1759	0.05978	0.1858
T_∞ (°R)	382.3	3.478	1.247	3.695
P_∞ (psia)	1.54	0.01114	0.005825	0.01257
Re/L (1/ft)	7.49e+06	8.01e+04	2.15e+04	8.30e+04
U_∞ (ft/sec)	6544	21.67	1.637	21.73
ρ_∞ (lbm/ft^3)	1.05e-02	7.94e-05	1.31e-05	8.05e-05
ρU_∞ (lbm/ft^2 s)	68.78	0.3379	0.08338	0.348

TABLE 7. ESTIMATED UNCERTAINTIES OF CALCULATED VALUES FOR DESIGN POINT 3

Parameter units	Nominal value	B	P	$U_{rss}\pm$
Mach	6.86	0.01173	0.0009603	0.01177
q_∞ (psia)	99.32	0.3351	0.05078	0.339
T_∞ (°R)	374.5	3.102	0.06897	3.103
P_∞ (psia)	3.014	0.01541	0.001936	0.01553
Re/L (1/ft)	1.54e+07	1.59e+05	7.00e+03	1.59e+05
U_∞ (ft/sec)	6620	21.25	0.1356	21.25
ρ_∞ (lbm/ft^3)	2.10e-02	1.53e-04	1.10e-05	1.53e-04
ρU_∞ (lbm/ft^2 s)	139	0.6509	0.0718	0.6548

TABLE 8. ESTIMATED UNCERTAINTIES OF MEASURED AND CALCULATED CONE DATA
FOR DESIGN POINT 1

Parameter units	Nominal value	B	P	U_{rss} ±
Pitot(psia)	47.5	0.424	0	0.848
Surface Press. Sta. 1 (psia)	11	0.174	0.0272	0.176
Cp	0.397	0.00782	0.001062	0.007893
P_w/P_∞	13.29	0.2727	0.03322	0.2747
Surface Press. Sta. 2-8 (psia)	4.5	0.174	0.0272	0.176
Cp	0.1433	0.006993	0.001062	0.007073
P_w/P_∞	5.436	0.2219	0.03292	0.2243
T_w (°F)	400	3	0.0196	3
Stanton No.	.0007-.0025	-	6% meas. value	6% meas. value

TABLE 9. ESTIMATED UNCERTAINTIES OF MEASURED AND CALCULATED CONE DATA
FOR DESIGN POINT 2

Parameter units	Nominal value	B	P	U_{rss} ±
Pitot(psia)	95	0.424	0	0.848
Surface Press. Sta. 1 (psia)	22	0.174	0.0272	0.176
Cp	0.3986	0.003916	0.000532	0.003952
P_w/P_∞	13.7	0.141	0.01698	0.142
Surface Press. Sta. 2-8 (psia)	9	0.174	0.0272	0.176
Cp	0.1445	0.003501	0.0005317	0.003542
P_w/P_∞	5.605	0.1145	0.01695	0.1157
T_w (°F)	500	3.75	0.0196	3.75
Stanton No.	.0007-.0022	-	6% meas. value	6% meas. value

TABLE 10. SHAKEOUT AND CALIBRATION RUN LOG, WTR 1622

Rake Runs							
Run #	Date	Mach#	Re/L x10⁶ /ft	P_H/P_0 psia	T_H/To °F	Pitot psia	Comments
2483	10/11	6.77	7.89	13300 5402	3100 2686	86.7	Flow Restrictor Characterization (FRC) Run 1
2484	10/12	6.70	5.22	13300 3784	3100 2802	61.4	FRC Run 2
2485	10/13	6.66	3.58	13300 2576	3100 2802	42.3	FRC Run 3, Cracks found in 5 hole restrictor, taken out of service
2486	11/18	6.72	5.91	13300 4078	3100 2783	65.4	1st run with one hole restrictor, repeat of FRC Run 2 achieved
2487	11/23	6.65	3.55	13300 2408	3100 2783	38	Repeat FRC Run 3 achieved with the one hole design
2488	11/30	6.81	10.6	17300 7728	3300 2851	121	FRC Run 4, achieved
2489	12/2	6.68	6.48	17300 5268	3400 3128	84	FRC Run 5, achieved
2490 2491	12/5 12/6	Both runs were attempts at Run 6 / 20 km design point. Both had a premature diaphragm burst just prior to the desired conditions.					
2492*	12/7	6.64	3.53	17300 2600	3300 2950	42.5	FRC Run 6; Design Point 1 Achieved, 20.5 km duplication
2493*	12/8	6.66	3.9	17300 2813	3300 2893	45.5	Repeat of 20 km point(2492)
2494	12/9	6.83	12.7	20200 10400	3300 3087	160	Unsuccessful run, control valve 3 oscillated, downstream flow restrictor liner collapsed
2495	12/12	6.8	12.4	20200 9700	3300 3000	153	FRC Run 7, Downstream Flow restrictor liner collapsed
2496*	12/13	6.71	7.23	20200 5531	3300 2989	88.2	Design Point 2 Achieved, 16 km duplication
2497*	12/14	6.75	7.28	20200 5641	3300 2982	87	Repeat Design point 2(2496) with the Pitot Rake in the aft location to define the core size
2498	12/15	6.66	3.5	17300 2673	3400 2992	42.6	Repeat Design point 1(2492) with the Pitot Rake in the aft location to define the core size
2501	1/6	Aborted Run due to problem with the heater control Inductrol unit 4-piece liner configuration was unsuccessful during the aborted run					
2502	1/12	Aborted Run due to high pressure leak in the diaphragm cavity line					
2503	1/13	6.82	11.7	20200 9153	3300 2985	142	Repeat of 2495, new TZM liner configuration was successful
2504	1/17	Aborted attempt at Design point 3; initial heater pressure too high					
2505	1/18	Aborted Run due to a software limit for heater permission interlock					
2506*	1/19	6.86	15.3	27000 11763	3400 2957	184	Design Point 3 Achieved, 11.5 km duplication

TABLE 10. SHAKEOUT AND CALIBRATION RUN LOG, WTR1622 (Continued)

Cone Runs							
Run # Date	Cone Pos.	Mach#	Re/L $\times 10^6$/ft	P_H/P_0 psia	T_H/T_o °F	Pitot psia	Comments
2507 2/9	0	6.75	7.38	20200 5670	3300 3061	92.1	6-inch Base Model, Design point 2
2508 2/10	0	6.73	3.94	17300 3107	3400 2994	47.4	6-inch Base Model, Design point 1
2509 2/15	0	6.78	7.7	20200 5869	3300 2950	90.5	9.25-inch Base/Full Model, Design point 2
2510 2/16	-2.5	6.62	4.00	17300 2967	3400 2971	48.8	9.25-inch Base Model off-centerline, Design point 1
2511 2/22	-2.5	6.70	8.1	20200 6093	3300 2976	98.7	9.25-inch Base Model off-centerline, Design point 2 , w/ BL Trip
2512 2/23	-2.5	6.62	4.01	17300 2883	3400 2912	47.8	Full Model off-centerline, Design point 1 , w/ BL Trip

* Design Point Condition

TABLE 11. RAKE CALIBRATION AVERAGE RUN CONDITIONS

Run #	P_0 psia	T_0 °F	Pitot psia	Mach	Pinf psia	Tinf deg R	Uinf ft/s	qinf psia	ρinf lbm/ft³	Reinf 10^6/ft	H_0 Btu/lbm	Run Time sec	Design Point-Approx. Altitude Duplication kft/km
2493	2821	2800	45.6	6.68	0.788	363	6353	24.62	0.0057	4.08	897	5	1-67kft/20.5km
2496	5521	2894	88.1	6.73	1.50	373	6486	47.58	0.0105	7.56	933	3	2-52kft/16km
2497*	5626	2870	87.8	6.77	1.47	366	6466	47.38	0.0105	7.67	926	3	2-52kft/16km
2498*	2721	2890	42.7	6.71	0.732	372	6450	23.07	0.0051	3.70	924	5	1-67kft/20.5km
2506	11849	2903	184	6.87	3.01	367	6573	99.63	0.0214	15.8	954	1.75	3-38kft/11.5km

* Rake positioned in aft location 15.75 in. downstream of the nozzle exit. All other runs rake is positioned at nozzle exit.

TABLE 12. CONE CALIBRATION AVERAGE RUN CONDITIONS.

Run #	P_0 psia	T_0 °F	Pitot psia	Mach	Pinf psia	Tinf deg R	Uinf ft/s	qinf psia	ρinf lbm/ft³	Reinf 10^6/ft	H_0 Btu/lbm	Cone Position	BL Trip	Design Point
2507	5934	2965	93.8	6.74	1.59	382	6565	50.67	0.0109	7.81	972	On		2
2508	3041	2878	49.3	6.66	0.855	375	6436	25.01	0.0060	4.25	921	On		1
2509	5864	2882	92.8	6.75	1.57	370	6479	50.09	0.0111	8.02	931	On		2
2510	2978	2891	48.3	6.66	0.839	377	6450	26.07	0.0058	4.13	925	2.5" Off		1
2511	6073	2879	96.0	6.76	1.62	369	6478	51.83	0.0114	8.32	930	2.5" Off	X	2
2512	2889	2833	46.9	6.67	0.814	369	6388	25.34	0.0058	4.13	907	2.5" Off	X	1

REFERENCES

1. Lafferty, J. F. and Marren, D. E., *NSWC Hypervelocity Tunnel 9 Mach 7 Thermal Structural Facility Verification and Calibration*, AIAA-95-00237, Jan 1995, Reno, NV.

2. Ragsdale, W.C. and Boyd, C.F.,*Hypervelocity Wind Tunnel 9 Facility Handbook, Third Edition*, NAVSWC TR 91-616, Jul 1993, Silver Spring, MD.

3. Harris, E.L. and Glowacki, W.J., *NOL Hypervelocity Wind Tunnel, Report No.1: Aerodynamic Design*, NOL TR 71-5, Silver Spring, MD.

4. Glowacki, W.J., *NOL Hypervelocity Wind Tunnel, Report No.2: Nozzle Design*, NOL TR 71-6, Silver Spring, MD.

5. NIST ITS-90, Table 5 for Tungsten-5% Rhenium versus Tungsten-26% Rhenium Thermocouples.

6. Lafferty, J. F., NSWC K24 memo, Subj: Calculation of Tunnel Conditions, Silver Spring, MD, 21 Nov 1994.

7. Boyd C. F. and Howell A., *Numerical Investigation of One-Dimensional Heat-Flux Calculations*, NSWCDD/TR-94/114, 25 Oct 1994, Silver Spring, MD.

8. AIAA, *Assessment of Wind Tunnel Data Uncertainty*, AIAA S-071-1995, April 1995

9. Kammeyer, M. E., NSWC K24 memo, Subj: Measurement Uncertainty for Tunnel 9, Version 2, 1 Jun 1995, Silver Spring, MD.

10. Coleman H. and Steele, W., *Experimentation and Uncertainty Analysis for Engineers,* John Wiley & Sons, NY, 1989.

11. Marren, D. E., *Hypervelocity Tunnel 9 Mach 10/14 Calibration*, NSWCDD/TR-92/160, 31 Jan 1994, Silver Spring, MD.

12. Swinford, N. F., *Hypervelocity Tunnel 9 Mach 8 Calibration*, NSWCDD/TR-93/40, Mar 1994, Silver Spring, MD.

13. Lederer, M. A., *Hypervelocity Wind Tunnel Number 9 High Mach Number Development Program*, NSWCDD/TR-94/96, 5 Dec 1994, Silver Spring, MD.

14. Richbourg, D. H., *A Three-Dimensional Boundary Layer Computer Program for Sphere-cone Type Re-entry Vehicles - Volume II Users Manual*, AFFDL-TR-78-67, Jun 1978, Philadelphia, PA.

Appendix A

Normalized Calculated Freestream Condition Tabular Data and Profiles

Tunnel 9 Thermal Structural Facility Flow Uniformity Calibration
Run 2493 (20 km Condition), Station 0.75 in.

Nominal Measured Freestream Conditions

Po	To	PT13	PT14
psia	degF	psia	psia
2821	2800	45.39	45.82

Nominal Calculated Freestream Conditions

PTave	MACH	qinf	Pinf	Tinf	RHOinf	Uinf	Re/L
psia		psia	psia	degR	lbm/ft^3	ft/sec	1/ft
45.605	6.68	24.62	0.788	363.6	0.00566	6353	4.08E+06

Profile Normalized to Nominal

Probe No.	Dist. from Centerline (in.)	PT	M	Qinf	Pinf	Tinf	RHOinf	Uinf	Re/L
PT23	-6.00	0.0116	2.5931	0.0117	0.0017	0.1627	0.0107	1.0458	0.0632
PT21	-5.50	0.1247	1.5829	0.1253	0.0500	0.4249	0.1177	1.0317	0.2685
PT19	-5.00	0.4302	1.2105	0.4312	0.2944	0.7051	0.4175	1.0164	0.5751
PT17	-4.50	0.7036	1.0841	0.7044	0.5995	0.8639	0.6938	1.0076	0.7912
PT15	-4.00	0.9378	1.0150	0.9380	0.9106	0.9736	0.9353	1.0015	0.9578
PT13*	-3.50	0.9952	1.0011	0.9953	0.9931	0.9980	0.9951	1.0001	0.9968
PT11	-3.00	0.9992	1.0002	0.9992	0.9988	0.9997	0.9992	1.0000	0.9994
PT9	-2.50	1.0189	0.9956	1.0189	1.0278	1.0079	1.0198	0.9996	1.0127
PT7	-2.00	1.0141	0.9968	1.0140	1.0206	1.0058	1.0147	0.9997	1.0094
PT5	-1.50	1.0055	0.9987	1.0055	1.0081	1.0023	1.0058	0.9999	1.0037
PT3	-1.00	1.0246	0.9944	1.0245	1.0362	1.0102	1.0257	0.9994	1.0165
PT1	-0.50	0.9978	1.0005	0.9978	0.9968	0.9991	0.9977	1.0001	0.9985
PT0	0.00	0.9463	1.0129	0.9464	0.9225	0.9772	0.9440	1.0013	0.9635
PT2	0.50	0.9806	1.0046	0.9807	0.9719	0.9919	0.9798	1.0005	0.9869
PT4	1.00	1.0304	0.9931	1.0302	1.0447	1.0125	1.0317	0.9993	1.0204
PT6	1.50	1.0315	0.9928	1.0314	1.0463	1.0130	1.0329	0.9993	1.0211
PT8	2.00	1.0140	0.9968	1.0140	1.0205	1.0058	1.0146	0.9997	1.0094
PT10	2.50	1.0306	0.9930	1.0305	1.0450	1.0127	1.0320	0.9993	1.0205
PT12	3.00	1.0164	0.9962	1.0164	1.0241	1.0068	1.0171	0.9996	1.0110
PT14*	3.50	1.0048	0.9989	1.0047	1.0069	1.0020	1.0049	0.9999	1.0032
PT16	4.00	0.9496	1.0121	0.9498	0.9273	0.9787	0.9475	1.0012	0.9658
PT18	4.50	0.6942	1.0873	0.6950	0.5879	0.8591	0.6842	1.0079	0.7842
PT20	5.00	0.4191	1.2175	0.4201	0.2835	0.6975	0.4064	1.0168	0.5656
PT22	5.50	0.1104	1.6244	0.1109	0.0421	0.4043	0.1040	1.0328	0.2492
PT24	6.00	0.0069	2.8230	0.0069	0.0009	0.1377	0.0063	1.0471	0.0440

* - averaged to determine nominal calculated freestream conditions

Tunnel 9 Thermal Structural Facility Flow Uniformity Calibration
Run 2493 (20 km Condition), Station 0.75 in.

Normalized Pitot or Dynamic Pressure

Normalized Mach No.

Normalized Pinf

Normalized Tinf

Normalized RHOinf

Normalized Uinf

Normalized Reynolds No.

Distance from Nozzle Centerline (in.)
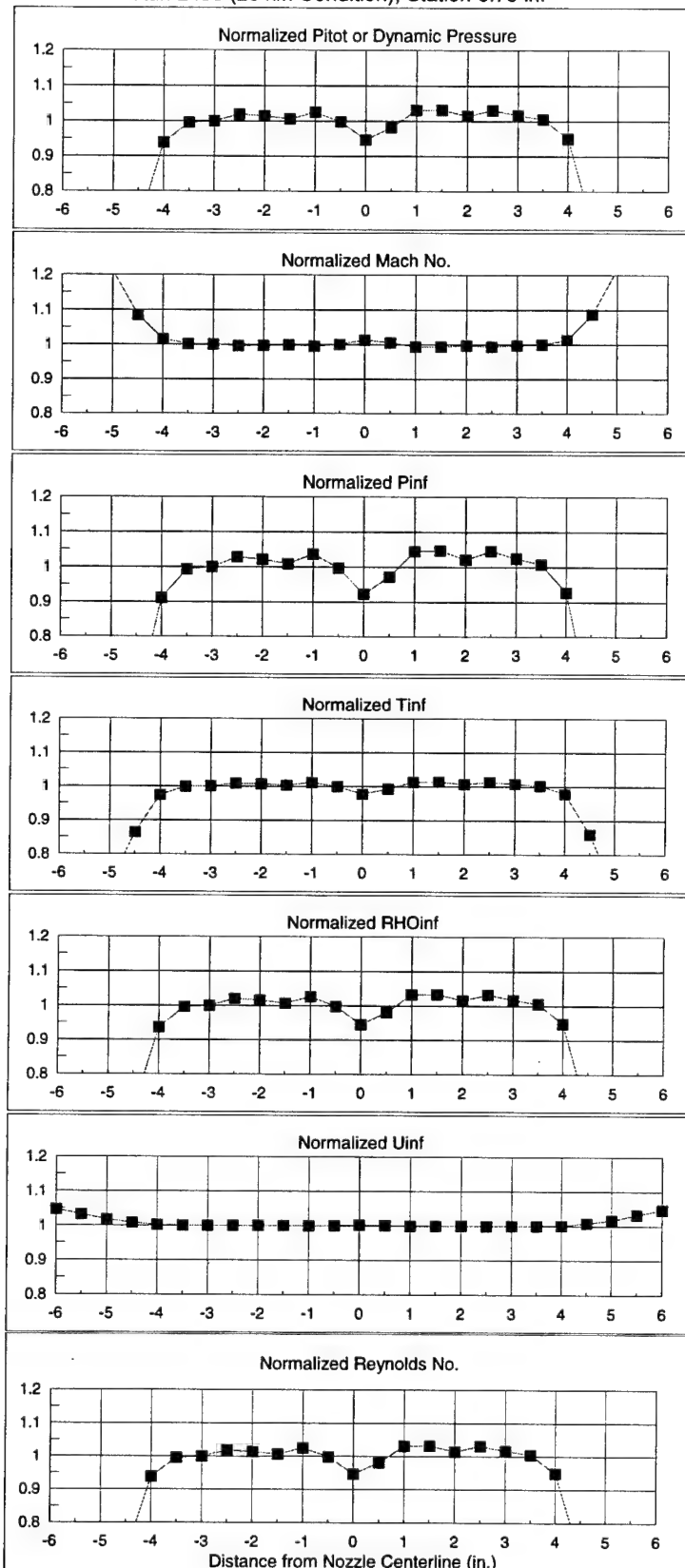
Tunnel 9 Thermal Structural Facility Flow Uniformity Calibration
Run 2498 (20 km Conditions) Station 15.0 in.

Nominal Measured Freestream Conditions

Po	To	PT5	PT6
psia	degF	psia	psia
2721	2890	42.68	42.78

Nominal Calculated Freestream Conditions

PTave	MACH	qinf	Pinf	Tinf	RHOinf	Uinf	Re/L
psia		psia	psia	degR	lbm/ft^3	ft/sec	1/ft
42.73	6.71	23.07	0.732	371.9	0.00514	6450	3.70E+06

Profile Normalized to Nominal

Probe No.	Dist. from Centerline (in.)	PT	M	qinf	Pinf	Tinf	RHOinf	Uinf	Re/L
PT23	-6.00	0.1570	1.5065	0.1577	0.0695	0.4668	0.1489	1.0292	0.3079
PT21	-5.50	0.2188	1.4028	0.2197	0.1116	0.5344	0.2089	1.0255	0.3770
PT19	-5.00	0.3085	1.3020	0.3095	0.1826	0.6151	0.2968	1.0211	0.4653
PT17	-4.50	0.4451	1.2011	0.4462	0.3093	0.7151	0.4325	1.0157	0.5868
PT15	-4.00	0.5958	1.1254	0.5968	0.4712	0.8065	0.5842	1.0107	0.7088
PT13	-3.50	0.7531	1.0673	0.7538	0.6618	0.8887	0.7446	1.0062	0.8271
PT11	-3.00	0.9301	1.0169	0.9304	0.8997	0.9703	0.9273	1.0017	0.9524
PT9	-2.50	1.0029	0.9993	1.0029	1.0042	1.0012	1.0030	0.9999	1.0019
PT7	-2.00	0.9931	1.0016	0.9931	0.9899	0.9971	0.9928	1.0002	0.9953
PT5*	-1.50	0.9988	1.0003	0.9989	0.9983	0.9995	0.9988	1.0000	0.9992
PT3	-1.00	1.0607	0.9864	1.0605	1.0900	1.0249	1.0635	0.9986	1.0407
PT1	-0.50	1.0169	0.9961	1.0168	1.0248	1.0070	1.0176	0.9996	1.0114
PT0	0.00	1.0065	0.9985	1.0065	1.0095	1.0027	1.0068	0.9999	1.0044
PT2	0.50	1.0029	0.9993	1.0029	1.0043	1.0012	1.0030	0.9999	1.0019
PT4	1.00	1.0483	0.9891	1.0481	1.0714	1.0199	1.0505	0.9989	1.0324
PT6*	1.50	1.0012	0.9997	1.0012	1.0017	1.0005	1.0012	1.0000	1.0008
PT8	2.00	0.9817	1.0043	0.9818	0.9734	0.9923	0.9809	1.0004	0.9876
PT10	2.50	0.9992	1.0002	0.9992	0.9989	0.9997	0.9992	1.0000	0.9995
PT12	3.00	0.9276	1.0175	0.9279	0.8963	0.9692	0.9247	1.0017	0.9507
PT14	3.50	0.7580	1.0657	0.7587	0.6680	0.8911	0.7496	1.0060	0.8307
PT16	4.00	0.5862	1.1295	0.5872	0.4603	0.8011	0.5745	1.0110	0.7013
PT18	4.50	0.4437	1.2020	0.4448	0.3079	0.7142	0.4311	1.0157	0.5856
PT20	5.00	0.3122	1.2987	0.3132	0.1857	0.6181	0.3005	1.0210	0.4687
PT22	5.50	0.2149	1.4082	0.2158	0.1088	0.5306	0.2051	1.0257	0.3729
PT24	6.00	0.1561	1.5082	0.1568	1.0292	0.4657	0.1481	1.0292	0.3069

* - averaged to determine nominal calculated freestream conditions

Run 2498 (20 km Conditions) Station 15.0 in.
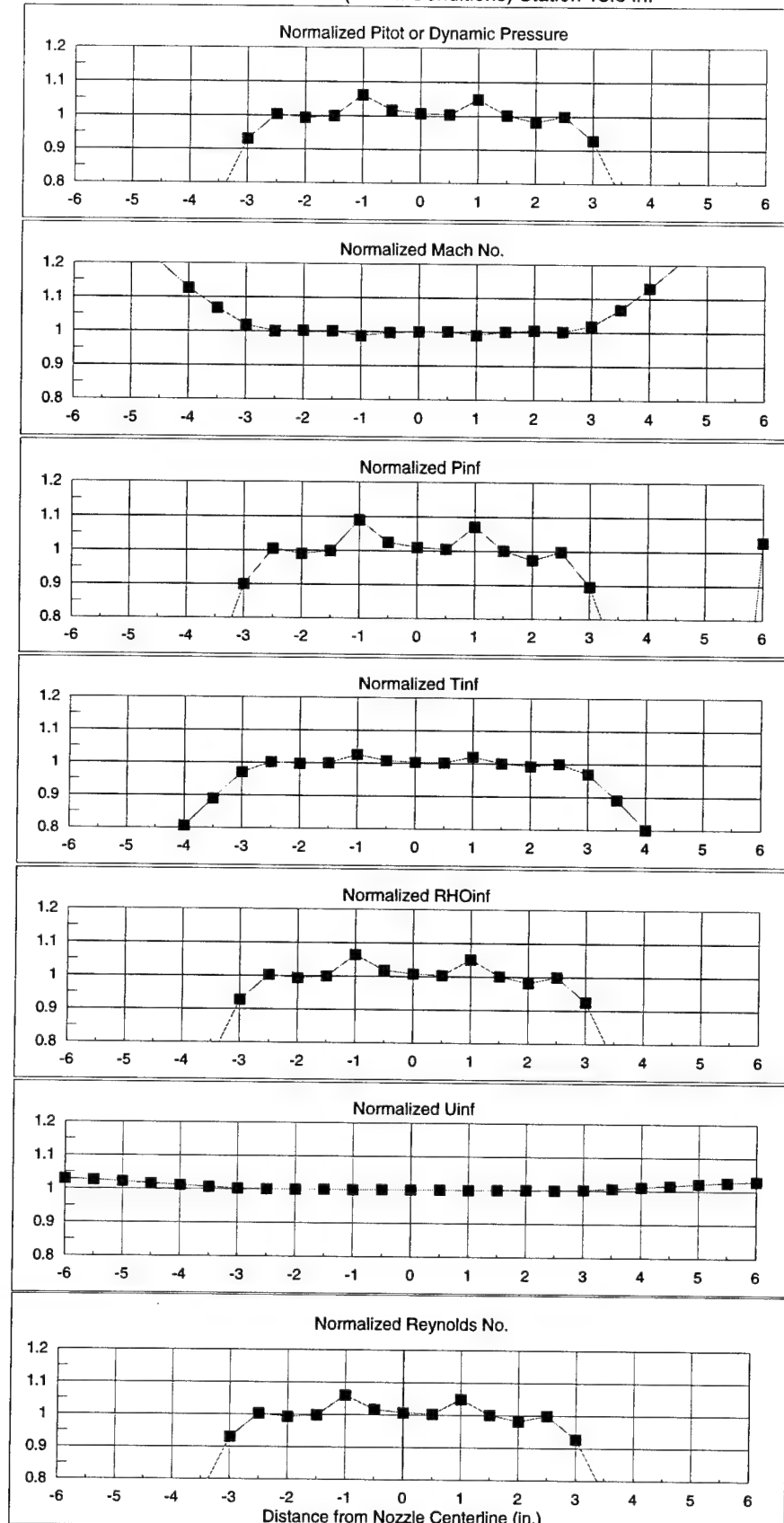
Normalized Pitot or Dynamic Pressure

Normalized Mach No.

Normalized Pinf

Normalized Tinf

Normalized RHOinf

Normalized Uinf

Normalized Reynolds No.

Distance from Nozzle Centerline (in.)

Tunnel 9 Thermal Structural Facility Flow Uniformity Calibration
Run 2496 (15 km Condition), Station 0.75 in.

Nominal Measured Freestream Conditions

Po	To	PT13	PT14
psia	degF	psia	psia
5521	2894	88.23	88

Nominal Calculated Freestream Conditions

PTave	MACH	qinf	Pinf	Tinf	RHOinf	Uinf	Re/L
psia		psia	psia	degR	lbm/ft^3	ft/sec	1/ft
88.115	6.73	47.58	1.499	373.4	0.01048	6486	7.56E+06

Profile Normalized to Nominal

| Probe No.	Dist. from Centerline (in.)	PT	M	qinf	Pinf	Tinf	RHOinf	Uinf	Re/L
PT23	-6.00	0.0083	2.7709	0.1426	0.0011	0.1426	0.0077	1.0462	0.0515
PT21	-5.50	0.1344	1.5572	0.4380	0.0557	0.4380	0.1271	1.0305	0.2799
PT19	-5.00	0.4531	1.1962	0.7204	0.3174	0.7204	0.4406	1.0153	0.5934
PT17	-4.50	0.7395	1.0717	0.8820	0.6446	0.8820	0.7308	1.0065	0.8171
PT15	-4.00	0.9658	1.0081	0.9856	0.9506	0.9856	0.9644	1.0008	0.9768
PT13*	-3.50	1.0013	0.9997	1.0006	1.0019	1.0006	1.0014	1.0000	1.0009
PT11	-3.00	0.9998	1.0000	0.9999	0.9998	0.9999	0.9998	1.0000	0.9999
PT9	-2.50	1.0079	0.9982	1.0033	1.0116	1.0033	1.0082	0.9998	1.0053
PT7	-2.00	1.0233	0.9946	1.0233	1.0343	1.0097	1.0243	0.9995	1.0157
PT5	-1.50	1.0143	0.9967	1.0143	1.0210	1.0059	1.0149	0.9997	1.0097
PT3	-1.00	0.9868	1.0031	0.9869	0.9808	0.9945	0.9863	1.0003	0.9911
PT1	-0.50	1.0142	0.9967	1.0142	1.0208	1.0059	1.0148	0.9997	1.0096
PT0	0.00	0.9552	1.0106	0.9554	0.9354	0.9811	0.9534	1.0010	0.9696
PT2	0.50	1.0085	0.9980	1.0085	1.0124	1.0035	1.0089	0.9998	1.0057
PT4	1.00	1.0014	0.9997	1.0014	1.0021	1.0006	1.0015	1.0000	1.0010
PT6	1.50	1.0084	0.9980	1.0084	1.0125	1.0035	1.0088	0.9998	1.0057
PT8	2.00	1.0242	0.9945	1.0241	1.0356	1.0100	1.0253	0.9994	1.0163
PT10	2.50	1.0257	0.9941	1.0256	1.0377	1.0106	1.0268	0.9994	1.0173
PT12	3.00	1.0102	0.9976	1.0102	1.0150	1.0043	1.0107	0.9998	1.0069
PT14*	3.50	0.9987	1.0003	0.9987	0.9981	0.9995	0.9987	1.0000	0.9991
PT16	4.00	0.9513	1.0116	0.9515	0.9298	0.9794	0.9494	1.0011	0.9669
PT18	4.50	0.7198	1.0783	0.7206	0.6198	0.8722	0.7106	1.0070	0.8026
PT20	5.00	0.4405	1.2037	0.4416	0.3048	0.7121	0.4280	1.0157	0.5827
PT22	5.50	0.1162	1.6057	0.1168	0.0453	0.4130	0.1097	1.0318	0.2562
PT24	6.00	0.0069	2.8588	0.0069	0.0008	0.1341	0.0063	1.0466	0.0449

* - averaged to determine nominal calculated freestream conditions

Tunnel 9 Thermal Structural Facility Flow Uniformity Calibration
Run 2496 (15 km Condition), Station 0.75 in.
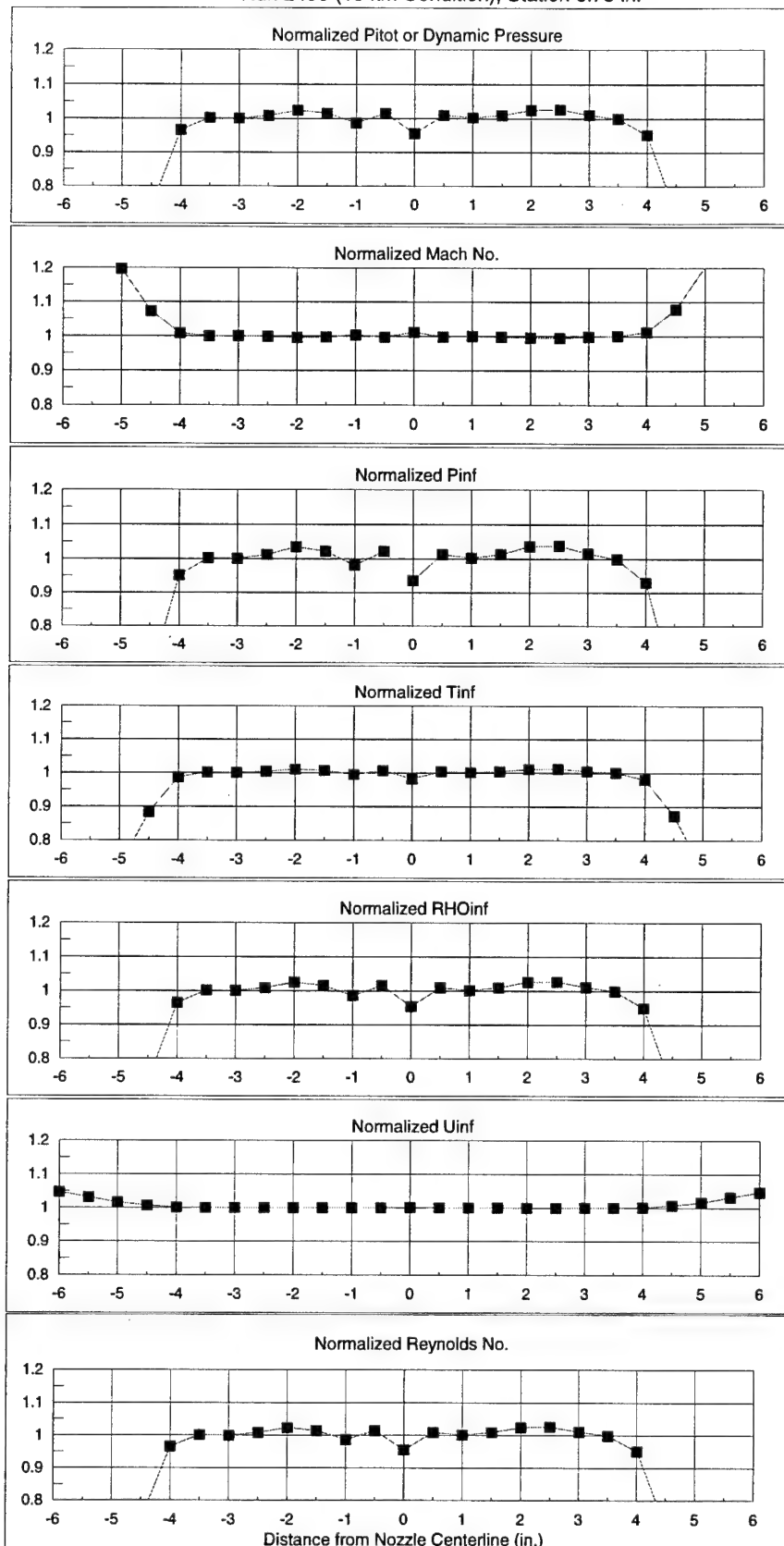
Tunnel 9 Thermal Structural Facility Flow Uniformity Calibration
Run 2497 (15 km Conditions) Station 15.0 in.

Nominal Measured Freestream Conditions

Po	To	PT5	PT6
psia	degF	psia	psia
5626	2870	86.66	88.84

Nominal Calculated Freestream Conditions

PTave	MACH	qinf	Pinf	Tinf	RHOinf	Uinf	Re/L
psia		psia	psia	degR	lbm/ft^3	ft/sec	1/ft
87.75	6.77	47.38	1.474	366.4	0.01051	6466	7.67E+06

Profile Normalized to Nominal

Probe No.	Dist. from Centerline (in.)	PT	M	qinf	Pinf	Tinf	RHOinf	Uinf	Re/L
PT23	-6.00	0.1601	1.4992	0.1608	0.4706	0.0715	0.1520	1.0284	0.3124
PT21	-5.50	0.2266	1.3914	0.2274	0.5423	0.1175	0.2167	1.0246	0.3861
PT19	-5.00	0.3250	1.2867	0.3260	0.6285	0.1969	0.3133	1.0200	0.4815
PT17	-4.50	0.4660	1.1886	0.4670	0.7288	0.3307	0.4536	1.0146	0.6050
PT15	-4.00	0.6107	1.1189	0.6116	0.8149	0.4886	0.5996	1.0100	0.7209
PT13	-3.50	0.7723	1.0611	0.7729	0.8981	0.6866	0.7645	1.0055	0.8414
PT11	-3.00	0.9502	1.0119	0.9503	0.9789	0.9282	0.9482	1.0011	0.9662
PT9	-2.50	1.0076	0.9982	1.0076	1.0032	1.0111	1.0079	0.9998	1.0051
PT7	-2.00	0.9931	1.0016	0.9931	0.9971	0.9900	0.9928	1.0002	0.9954
PT5*	-1.50	0.9876	1.0029	0.9877	0.9948	0.9820	0.9871	1.0003	0.9916
PT3	-1.00	1.0111	0.9974	1.0110	1.0046	1.0162	1.0116	0.9997	1.0075
PT1	-0.50	1.0725	0.9839	1.0723	1.0296	1.1078	1.0758	0.9984	1.0484
PT0	0.00	1.0370	0.9916	1.0369	1.0153	1.0545	1.0386	0.9992	1.0248
PT2	0.50	1.0327	0.9926	1.0326	1.0135	1.0482	1.0341	0.9993	1.0219
PT4	1.00	1.0367	0.9917	1.0366	1.0152	1.0541	1.0383	0.9992	1.0246
PT6*	1.50	1.0124	0.9971	1.0124	1.0052	1.0182	1.0130	0.9997	1.0084
PT8	2.00	0.9883	1.0027	0.9883	0.9951	0.9830	0.9878	1.0003	0.9921
PT10	2.50	1.0107	0.9976	1.0106	1.0044	1.0156	1.0111	0.9998	1.0072
PT12	3.00	0.9588	1.0097	0.9590	0.9826	0.9406	0.9572	1.0009	0.9721
PT14	3.50	0.7785	1.0591	0.7792	0.9011	0.6947	0.7709	1.0054	0.8459
PT16	4.00	0.6100	1.1192	0.6109	0.8145	0.4878	0.5989	1.0100	0.7203
PT18	4.50	0.4636	1.1899	0.4647	0.7273	0.3282	0.4513	1.0147	0.6031
PT20	5.00	0.3246	1.2870	0.3256	0.6282	0.1966	0.3129	1.0200	0.4811
PT22	5.50	0.2218	1.3979	0.2226	0.5375	0.1139	0.2119	1.0249	0.3810
PT24	6.00	0.1602	1.4989	0.1609	0.4708	0.0716	0.1521	1.0284	0.3125

* - averaged to determine nominal calculated freestream conditions

Tunnel 9 Thermal Structural Facility Flow Uniformity Calibration
Run 2497 (15 km Conditions) Station 15.0 in.

Normalized Pitot or Dynamic Pressure

Normalized Mach No.

Normalized Pinf

Normalized Tinf

Normalized RHOinf

Normalized Uinf

Normalized Reynolds No.

Distance from Nozzle Centerline (in.)
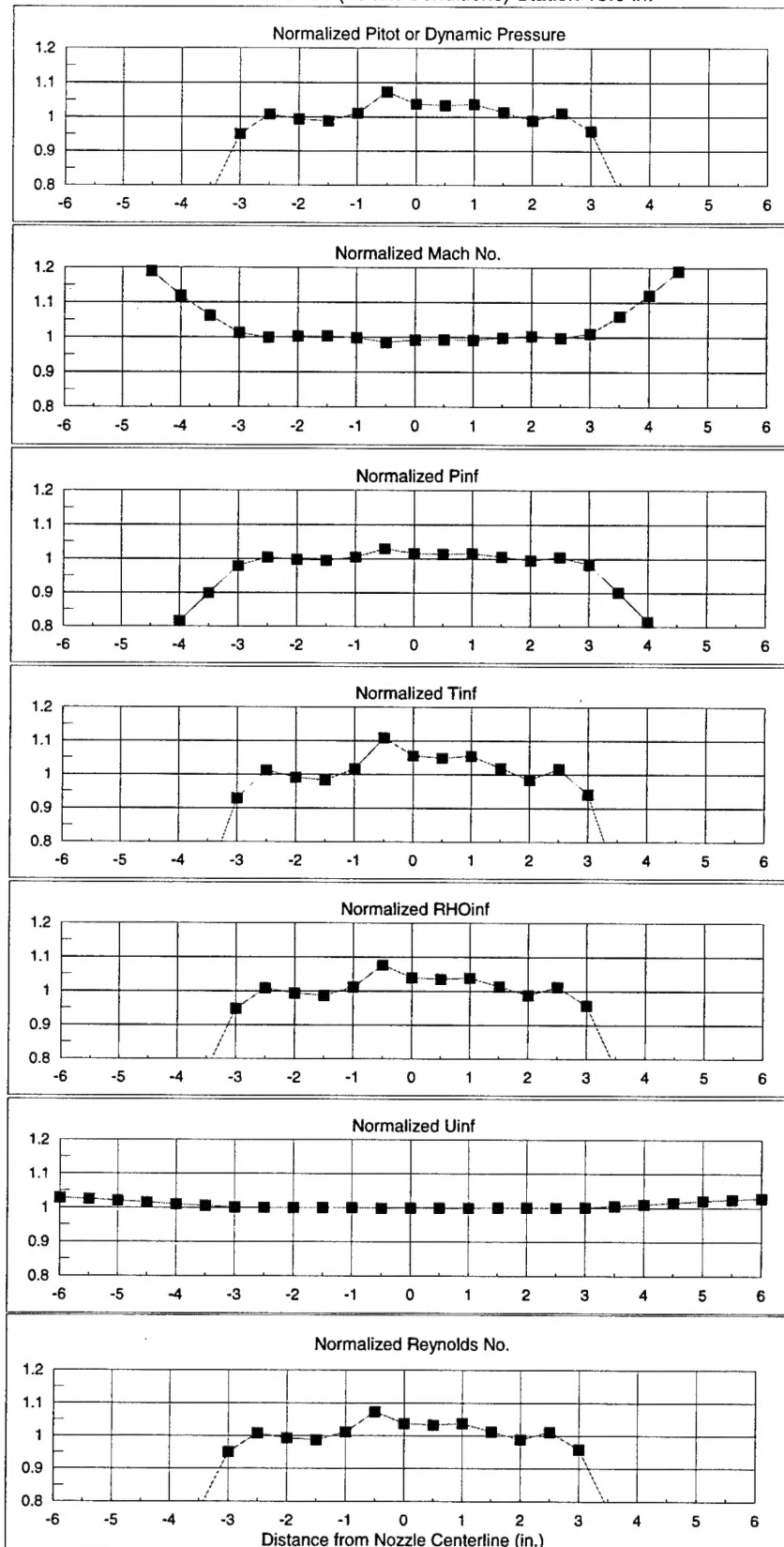
Tunnel 9 Thermal Structural Facility Flow Uniformity Calibration
Run 2506, Station 0.75 in.

Nominal Measured Freestream Conditions

Po	To	PT13	PT14
psia	degF	psia	psia
11819	2903	184.37	184.49

Nominal Calculated Freestream Conditions

PTave	MACH	qinf	Pinf	Tinf	RHOinf	Uinf	Re/L
psia		psia	psia	degR	lbm/ft^3	ft/sec	1/ft
184.43	6.87	99.63	3.008	367.4	0.02137	6573	1.58E+07

Profile Normalized to Nominal

Probe No.	Dist. from Centerline (in.)	PT	M	Qinf	Pinf	Tinf	RHOinf	Uinf	Re/L
PT23	-6.00	0.0075	2.8225	0.0075	0.0009	0.1370	0.0069	1.0446	0.0481
PT21	-5.50	0.1329	1.5584	0.1334	0.0550	0.4364	0.1260	1.0293	0.2788
PT19	-5.00	0.4648	1.1887	0.4657	0.3297	0.7282	0.4527	1.0143	0.6039
PT17	-4.50	0.7364	1.0724	0.7371	0.6410	0.8806	0.7279	1.0063	0.8152
PT15	-4.00	0.9588	1.0097	0.9590	0.9406	0.9826	0.9572	1.0009	0.9721
PT13*	-3.50	0.9997	1.0001	0.9997	0.9996	0.9999	0.9997	1.0000	0.9998
PT11	-3.00	1.0096	0.9978	1.0096	1.0141	1.0040	1.0101	0.9998	1.0065
PT9	-2.50	1.0248	0.9943	1.0248	1.0364	1.0103	1.0259	0.9995	1.0167
PT7	-2.00	1.0291	0.9934	1.0291	1.0428	1.0120	1.0304	0.9994	1.0196
PT5	-1.50	0.9798	1.0047	0.9799	0.9707	0.9915	0.9790	1.0004	0.9864
PT3	-1.00	0.9990	1.0003	0.9990	0.9985	0.9996	0.9989	1.0000	0.9993
PT1	-0.50	1.0677	0.9849	1.0676	1.1004	1.0277	1.0707	0.9985	1.0453
PT0	0.00	1.0359	0.9919	1.0358	1.0529	1.0148	1.0375	0.9992	1.0241
PT2	0.50	1.0755	0.9833	1.0753	1.1121	1.0308	1.0788	0.9984	1.0504
PT4	1.00	1.0043	0.9990	1.0043	1.0062	1.0018	1.0044	0.9999	1.0029
PT6	1.50	0.9810	1.0044	0.9810	0.9724	0.9920	0.9802	1.0004	0.9871
PT8	2.00	1.0029	0.9993	1.0029	1.0043	1.0012	1.0030	0.9999	1.0020
PT10	2.50	1.0423	0.9905	1.0422	1.0623	1.0174	1.0441	0.9991	1.0283
PT12	3.00	1.0107	0.9975	1.0107	1.0157	1.0044	1.0111	0.9998	1.0072
PT14*	3.50	1.0003	0.9999	1.0003	1.0005	1.0001	1.0003	1.0000	1.0002
PT16	4.00	0.9792	1.0048	0.9793	0.9698	0.9913	0.9784	1.0005	0.9859
PT18	4.50	0.7593	1.0649	0.7600	0.6702	0.8919	0.7514	1.0057	0.8320
PT20	5.00	0.4574	1.1929	0.4584	0.3222	0.7234	0.4454	1.0145	0.5978
PT22	5.50	0.1211	1.5893	0.1216	0.0482	0.4202	0.1146	1.0302	0.2634
PT24	6.00	0.0067	2.8310	0.0067	0.0008	0.1362	0.0061	1.0446	0.0431

* - averaged to determine nominal calculated freestream conditions

Tunnel 9 Thermal Structural Facility Flow Uniformity Calibration
Run 2506, Station 0.75 in.
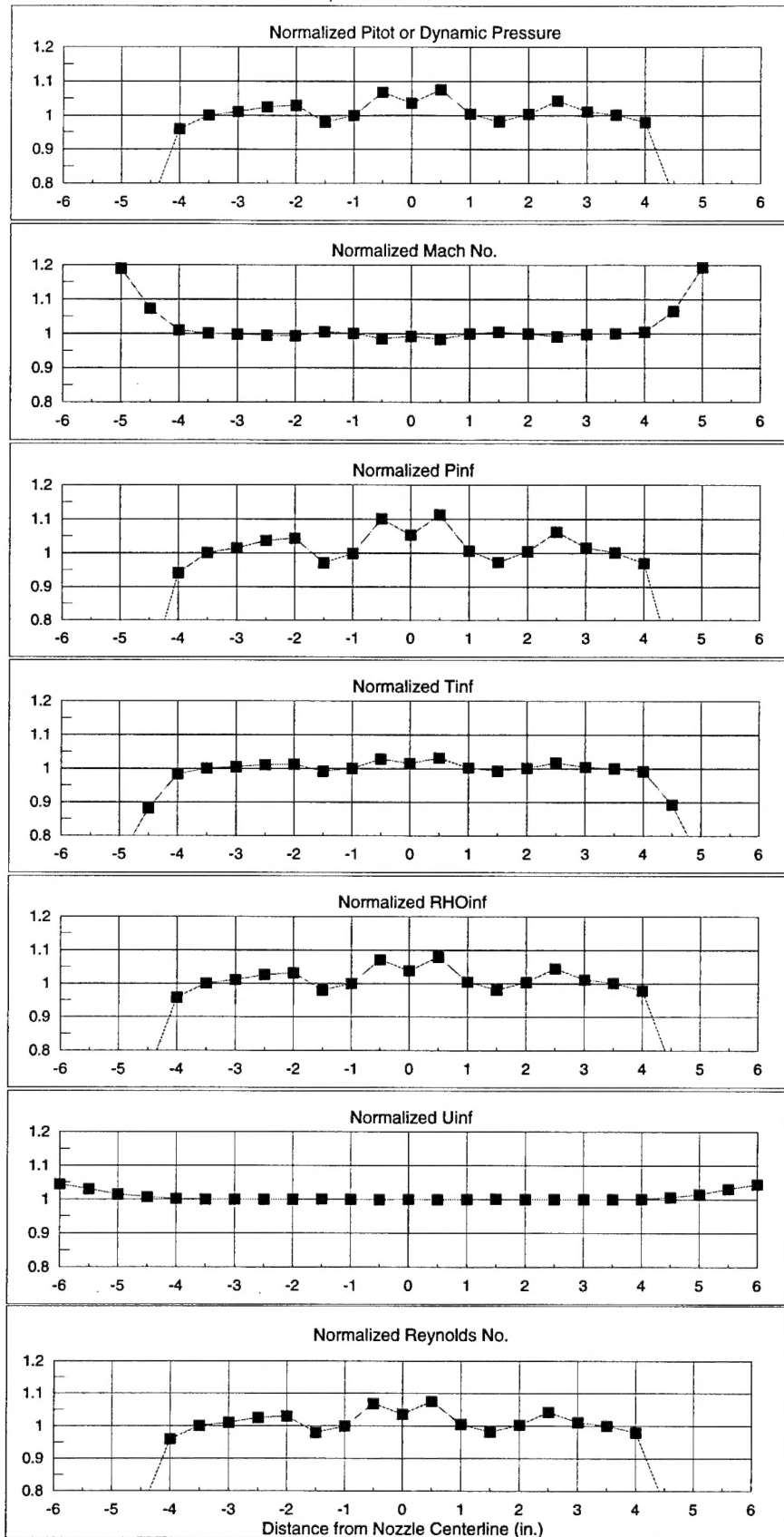
DISTRIBUTION

	Copies		Copies

DOD ACTIVITIES (CONUS)

ATTN JOHN LAFFERTY   41
AEDC WHITE OAK
10905 NEW HAMPSHIRE AVENUE
SILVER SPRING MD 20903-1050

ATTN CODE A76 (TECHNICAL LIBRARY) 1
COMMANDING OFFICER
CSSDD NSWC
6703 W HIGHWAY 98
PANAMA CITY FL 32407-7001

DEFENSE TECHNICAL INFORMATION CTR
8725 JOHN J KINGMAN ROAD
SUITE 0944
FT BELVOIR VA 22060-6218   2

NON-DOD ACTIVITIES (CONUS)

THE CNA CORPORATION
P O BOX 16268
ALEXANDRIA VA 22302-0268   1

INTERNAL

B60 (TECHNICAL LIBRARY)   3